UNIVERSITY OF CALIFORNIA, SAN DIEGO

# fMRI Representation of Transient Onsets and Adaptation

A dissertation submitted in partial satisfaction of the

Requirements for the degree of Doctor of Philosophy

in

Neurosciences

by

August Saul Tuan

Committee in charge:

Professor Geoffrey M. Boynton, Chair
Professor Richard B. Buxton, Co-Chair
Professor Karen R. Dobkins
Professor Thomas T. Liu
Professor John H. Reynolds

2006

The dissertation of August Saul Tuan is approved, and it is acceptable in quality and form for publication on microfilm:

_____

_____

_____

_____
Co-Chair

_____
Chair

University of California, San Diego

2006

Dedicated to

my parents Fang-jen and Chuan-tai Tuan

for their unconditional love, support, and encouragement.

TABLE OF CONTENTS

LIST OF FIGURES

ACKNOWLEDGEMENTS

I have been fortunate to work with Geoff Boynton and receive his mentorship, guidance, and friendship. His enthusiasm and support have made my work in the lab wonderful and allowed me to focus on what I'm what I'm most excited about: fMRI. More importantly, Geoff has taught me how to approach scientific questions and think more critically as a scientist, and I am truly grateful and indebted for that. I only hope that I can one day properly use these tools I have been given in my own academic career, perform great science, and justify the mentoring that Geoff has invested in my training.

I wish to thank the members of the Boynton lab Vivian Ciaramitaro, Sara Mednick, John Serences, and of course, my partner in crime and fellow graduate student Minna Ng for their help on my project and camaraderie. Vivian and Minna have been especially helpful me as scanning buddies and subjects and giving me intellectual input into my project. A deep debt of gratitude also goes to members of the lab for putting up with my nonstop whooping cough in the waning months of my graduate career.

I'd like to thank the alums of the Boynton lab who trained me and helped me to grow as a graduate student: Cyrus Arman, Eva Finney, Rob Duncan, Ed Hubbard, and Giedrius Buracas. Special thanks to Melissa Saenz who helped me early in my graduate career and was the graduate student whom I strived to emulate but whose shoes I could never possibly fill.

I am grateful for the training and mentoring I received from Peter Bandettini and Rasmus Birn as well as the rest of the Functional Imaging Methods Unit at the National Institutes of Mental Health when I spent my wonderful year at the NIH. Peter and Rasmus gave me my first opportunity to operate a 3T scanner and in the process made me a more competent operator when I returned to UCSD.

I am thankful for the advice and thought-provoking questions my committee members asked me to further strengthen my thesis: Richard Buxton, Karen Dobkins, John Reynolds, and Tom Liu. I am honored to have them on my dissertation committee.

Special thanks to Ione Fine for teaching me how to program in Matlab and think like a programmer when I was a mere coding noob early on in my graduate career.

I want to thank my family for their love and giving me a wonderful childhood. While we did not have much materially when I was growing up, I learned there

are many things more valuable than possessions. My father piqued my excitement for science early and nourished my curiosity to learn how things worked. My mother has been an inspiration to me through her diligence, sacrifice, and showing me how to make lemonade whenever you are in a lemon of a situation.

The text of Chapter Two is a reprint of a manuscript submitted for publication of which I am the primary author. It has been submitted as August S. Tuan, Rasmus M. Birn, Peter A. Bandettini, and Geoffrey M. Boynton. "Differential transient MEG and fMRI responses to visual stimulation onset rate." *Neuroimage*. 2006.

The text of Chapter Three is a reprint of a manuscript being prepared for submission of which I am the primary author. It will be submitted as August S. Tuan and Geoffrey M. Boynton. "fMRI Adaptation to Motion in Human Visual Areas is reflected in Behavioral Performance." *Journal of Neurophysiology*. 2006.

My coauthors on these manuscripts have provided permission for material to be reproduced in this dissertation.

# VITA

| | |
|---|---|
| 1999 | B.S., Chemistry with High Distinction,<br>Harvey Mudd College |
| 1999-2008 | Medical Scientist Training Program,<br>University of California, San Diego |
| 2006 | Ph.D.in Neurosciences,<br>University of California, San Diego |

## PUBLICATIONS

Tuan, A, Birn, RM, Bandettini, P, Boynton, GM. “Differential transient MEG and fMRI responses to visual stimulation onset rate.” *Neuroimage*. Submitted.

## ABSTRACTS

August S. Tuan, Rasmus M. Birn, Geoffrey M. Boynton, Peter A. Bandettini. Talk. “Is the BOLD nonlinearity due to a transient in the neuronal response?,” 2004 Society for Neurosciences Conference, San Diego, CA.

August S. Tuan, Rasmus M. Birn, Geoffrey M. Boynton, Peter A. Bandettini. Poster presentation. “Non-linear Onset MEG Response in Ramped Stimuli in V1 suggests BOLD Nonlinearity is Neuronal in Origin,” 2004 Human Brain Mapping Conference, Budapest, Hungary.

August S. Tuan, Rasmus M. Birn, Geoffrey M. Boynton, Peter A. Bandettini. Poster presentation. “Non-linear Response to Ramped Onset Stimuli in V1,” 2003 Human Brain Mapping Conference, New York, NY.

## PROFESSIONAL EXPERIENCE

2005 Reviewer for Neuroimage

## TEACHING EXPERIENCE

2004 Small Group Facilitator for Basic Neurology, UCSD School of Medicine

HONORS AND FELLOWSHIPS

| | |
|---|---|
| 2005-2006 | Aginksy Endowment Scholarship |
| 2004-2005 | Salk Institute Association Scholarship |
| 2003-2004 | Merck Fellowship |
| 2004 | Travel Award for the Human Brain Mapping Conference, Budapest, Hungary |
| 2002-2003 | National Institutes of Health Undergraduate Scholarship for Individuals with Disadvantaged Backgrounds |
| 2001 | Honors in Introduction to Clinical Medicine |
| 2000 | Honors in Epidemiology and Biostatistics |

PROFESSIONAL AFFLIATIONS

Society for Neuroscience

The Organization for Human Brain Mapping

Vision Sciences Society

American Medical Association

California Medical Association

## ABSTRACT OF THE DISSERTATION

fMRI Representation of Transient Onsets and Adaptation

by

August Saul Tuan

Doctor of Philosophy in Neurosciences

University of California, San Diego, 2006

Professor Geoffrey M. Boynton, Chair

Professor Richard B. Buxton, Co-Chair

Functional magnetic resonance imaging (fMRI) has become a powerful tool to noninvasively localize and measure in vivo brain function, and the growth of the field has exploded. However, the strength and validity of the technique lies in understanding the relationship between the underlying neuronal activity and the fMRI signal. While we know that the fMRI signal increases in response to metabolic demands of increased neuronal activity, we do not understand the exact relationship between neural activity,

hemodynamics, and the fMRI signal. The fMRI response is known to be nonlinear and disproportionately large at short stimulus durations. This dissertation examines the nonlinearity of the fMRI signal and how we may utilize a nonlinear response to understand neuronal populations on a subvoxel level. First, the hypothesis of transient neuronal onsets as a source of fMRI nonlinearity at short stimulus durations was examined using MEG and fMRI. We observed that transient neuronal activity is not the sole source of fMRI nonlinearity. Second, the validity of the fMRI adaptation paradigm was assessed by examining a well-known adaptive property (motion) in well-studied visual areas. These results were compared with psychophysical performance on a speed discrimination task and imply that MT+ is direction selective while visual areas V1, V2, V3, V3A, and V4V are orientation selective.

# Chapter 1

# Introduction

### 1.1 Proliferation of fMRI

Functional magnetic resonance imaging (fMRI) has only existed for approximately fifteen years, but it has dramatically revolutionized cognitive neuroscience since its inception. Taking advantage of a quirk in nature through the differential magnetization of hemoglobin and deoxyhemoglobin, creating detectable local field inhomogenities, fMRI can non-invasively localize and measure in vivo brain activity. This has allowed fMRI to be utilized as an extremely powerful tool to study human brain function in parallel to invasive electrophysiological recordings in non-human primates and other mammals. As a result, the number of fMRI groups, studies, and papers has mushroomed in the last decade with a diverse array of experiments investigating elementary fingertaping in the motor cortex (Bandettini et al. 1993; Rao et al. 1993) to more higher level concepts like love (Aron et al. 2005). The number of fMRI articles has increased by about 150 more peer-reviewed articles published than the preceding year with approximately 60 articles in 1994 and nearly 900 publications by 2001(Illes et al. 2003).

### 1.2 The source of the fMRI signal is not well understood

Nevertheless, the validity of fMRI lies in the relationship between the fMRI signal and the underlying neuronal activity. Many groups simply assume

that the fMRI signal is linear with respect to neuronal activity because it simplifies fMRI data analysis and allows the inference that a change in fMRI signal is neuronal in origin. However, while the fMRI signal is elicited by metabolic demands of increased neuronal activity and changes in deoxyhemoglobin concentration are dependent on a complex interaction between cerebral metabolic rate of oxygen ($CMRO_2$), cerebral blood flow (CBF), and cerebral blood volume (CBV), the exact relationship between neuronal activity, this complex interaction of hemodynamics and the fMRI signal are not clear. It is imperative that a clear understanding and validation of fMRI is needed to properly analyze and interpret the signals we are measuring, otherwise we are not sure what we are measuring exactly and the weight and significance of neuronal interpretations of fMRI studies is greatly diminished.

### 1.3 Controversies in fMRI

In addition to not knowing what the precise relationship between neuronal activity and the fMRI signal, the current climate of the fMRI community is slightly akin to the Wild Wild West as researchers struggle and debate over the most optimal methodology in fMRI. There are debates over stimulus presentation paradigms (Birn and Bandettini 2005; Buckner 1998; Buracas and Boynton 2002; Dale and Buckner 1997), data analysis packages (Cox 1996; Friston et al. 1991; Goebel et al. 2006; Penny and Friston 2003),

and even the validity of using functional localizers to restrict regions of interests (Friston and Henson 2006; Friston et al. 2006; Saxe et al. 2006).

One of the biggest controversies lies in whether the fMRI signal is reflective of spiking output activity or input intracortical processing. A couple of groups compared monkey single-unit data to human fMRI signals and concluded that fMRI signals were directly proportional to average neuronal firing rates (Boynton et al. 1999; Geisler and Albrecht 1997; Heeger et al. 2000; Rees et al. 2000). One caveat of these studies is that neuronal activity and fMRI signals were studied from different brains and across two different species. However, a remarkable study simultaneously recorded fMRI signals and neuronal activity in an anesthetized macaque (Logothetis et al. 2001). They found that the fMRI signals did not correlate best with neuronal activity but with local field potential. Since local field potentials are believed to reflect the superposition of synchronized dendritic currents average over a large volume of tissue (Heeger and Ress 2002), Logothetis interpreted that the fMRI signals therefore “reflect the input and intracortical processing of a given area rather than its spiking output.” The intracortical processing hypothesis is supported by a study which utilized a special cerebellar circuit which excited inhibitory interneurons but did not result in output spiking in Purkinje cells, however, both blood flow and local field potential increased (Mathiesen et al. 1998).

### 1.4 Linear systems theory

A way to determine if the fMRI response is representative of the input stimulus presented to subjects is to see if the fMRI system is linear. If the fMRI response is found to be linear, this would simplify our stimulus design and data analysis. An fMRI response that is linear with respect to the stimulus potentially allows for a complex nonlinear neuronal transformation of the stimulus and a nonlinear hemodynamic transformation of the neuronal response. To truly assess the linearity of the fMRI signal to neuronal activity, one must measure electrophysiological activity.

A system is considered linear if it obeys two properties; it must be proportional and additive. If a stimulus generates a particular response, and doubling the intensity of the stimulus increases the response two-fold, then the system is proportional. If the response to the sum of two stimuli equals the sum of the responses to the same two stimuli, then the system is additive. If both of these conditions are met, then the system is considered linear. That means in a linear system, it is possible to predict the response to a long stimulus by summing the response to shorter stimuli (Boynton et al. 1996).

### 1.5 Nonlinearity of fMRI

A number of studies have tested the linearity of the fMRI response (Boynton et al. 1996; Miller et al. 2001; Robson et al. 1998; Vazquez and Noll 1998). In stimulus durations greater than six seconds, the linearity of the fMRI response holds up well, however, when the stimulus duration decreases to 3

seconds or less, the fMRI response becomes nonlinear (Boynton et al. 1996). Short duration stimuli have a disproportionately larger fMRI response than would be expected in a linear system.

### 1.6 Sources of nonlinearity

A number of hypotheses have been formulated to explain the nonlinearity of the fMRI response at short stimulus durations. A neuronal origin of fMRI nonlinearity may be neural adaptation through the presence of transient onset activity. Electrophysiological recordings of macaque V1 presented with a grating show a rapid rise in neuronal activity followed by a quick decay (~100 msec) to a steady-state firing rate (Muller et al. 2001, 1999). Perhaps at short stimulus durations, the fMRI response is being disproportionately driven by the large and rapid transient neuronal activity at the onset of a stimulus. Longer stimulus durations may show less nonlinearity as the relatively larger contribution from steady-state neuronal firing dilutes the response to transient activity. Long-term neuronal adaptation may also be contribute to this nonlinearity as V1 responses decrease after prolonged (4 – 30 second) stimuluation (Ohzawa et al. 1985). A vascular source of fMRI nonlinearity may lie in a nonlinear relationship between the fMRI response and flow (Heeger and Ress 2002; Mechelli et al. 2001; Miller et al. 2001).

### 1.7 Applications of nonlinearity

While having a nonlinear fMRI response may seem like a detriment to understanding what the fMRI signal represents on a neuronal level, we may be

able to use this situation to our advantage to investigate brain function on a subvoxel level. A number of studies have begun to use a nonlinear fMRI response to tease out neuronal subpopulations on resolutions below that of a typical fMRI voxel through an adaptation paradigm (Grill-Spector et al. 1999; Grill-Spector and Malach 2001). The assumption is that the presentation of a stimulus will adapt, or fatigue, neurons which respond to the stimulus, and the repeated presentation of the same stimulus will yield a weaker response. If the adapting stimulus is presented and a second stimulus, transformed along some stimulus dimension, is presented and the response is equally weak, it is inferred that neuronal subpopulations are not sensitive to the change in stimulus dimension. If, however, the response is larger resulting in a release of adaptation, it is inferred that neuronal subpopulations are sensitive to the change in stimulus dimension. While a number of studies in higher areas are utilizing this new paradigm to elucidate neuronal subpopulations, it is not well-known whether this paradigm is revealing adaptation in neuronal subpopulations or is reflecting hemodynamic refractoriness. A study using well-known adaptive properties in well-studied cortical areas is needed before we can make strong inferences in less-studied higher areas.

### 1.8 Description of manuscripts

In this dissertation, we investigate the linearity of the fMRI response and characterize motion-specific fMRI adaptation. One of the first things to check in the fMRI response is to see if it is linear because that would simplify

fMRI design and data analysis. However, it is known that the fMRI response to short duration stimuli is much larger than expected in a linear system. One possible explanation is that the presence of transient neuronal firing at the onset of the stimulus outweighs the sustained neuronal response and is the source of this nonlinearity at short stimulus durations. We explore this hypothesis using MEG and fMRI. fMRI adaptation has been used to reveal neuronal subpopulations within resolutions smaller than a typical fMRI voxel. The technique relies on the assumption that neurons sensitive to a particular stimulus or stimulus dimension will fatigue after a presentation. Thus, repeated presentation of the same stimulus should yield a weaker response while presentation of a stimulus transformed on a particular stimulus dimension should excite a new, unadapted subpopulation of neurons and yield a larger response. Observation of this release in adaptation would imply that neuronal subpopulations sensitive to changes in the particular stimulus dimension exist. While many studies have employed this technique to make inferences about higher order areas, little is known about the validity of the technique using a well studied adaptive property in well-studied cortical areas. In addition, many groups only assume that fMRI adaptation is a result of either neuronal or hemodynamic effects but do not usually consider both. We used an event-related fMRI study to examine motion-specific adaptation in visual areas V1, V2, V3, V3A, V4V, and MT+. The original goal was to study these effects in combination with electrophysiological recordings to make stronger

inferences about neuronal activity. However, due to unfortunate circumstances, that was not possible so these results were compared to a human psychophysical experiment which assessed speed discrimination thresholds in a similar paradigm.

Chapter Two presents data examining one hypothesis behind the nonlinearity of the fMRI signal at short stimulus durations. Nearly all methods of fMRI stimulus presentation, data analysis, and interpretation assume that BOLD fMRI signal is linear with respect to the underlying neuronal response. However, short stimulus durations are known to produce a much larger fMRI response than expected form a linear system. This nonlinearity in the response has been hypothesized to be caused by neuronal onset and offset transients instead of hemodynamic nonlinearity. We tested this hypothesis in chapter Two by measuring MEG and fMRI responses to stimuli with ramped contrast onsets and offsets substituting the abrupt transitions. We first utilized the high temporal resolution of MEG to observe the response in visual cortex which showed that utilizing a ramped contrast transition decreases the transient activity. However, our fMRI results show no change in amount of nonlinearity in the response to the ramped contrast transition. Using the MEG response as a surrogate for neuronal activity, we predicted an fMRI response to the ramped stimuli. The MEG-derived fMRI predictions show a nonlinearity associated with short stimulus durations, but this nonlinearity is much smaller

than the observed nonlinearity in the BOLD signal. We therefore conclude that the BOLD nonlinearity is not solely due to transient onset activity.

Chapter Three is a study examining the neuronal and vascular contributions of an fMRI adaptation paradigm with respect to motion-selectivity in visual areas V1, V2, V3, V3A, V4V, and MT+. There have been numerous studies using an fMRI adaptation paradigm to selectivity isolate neuronal subpopulations with resolutions lower than typical fMRI voxels. Many studies have show robust results using fMRI adaptation, but others show strikingly null results for orientation-selectively in V1 which has a vast amount of electrophysiological evidence for orientation-selective cells. This conundrum posits the question of what we are exactly measuring in fMRI adaptation paradigms. Is it possible that signals in fMRI adaptation do not reflect expected neuronal adaptation but actually represent a hemodynamic refractoriness or recruitment of fresh vasculature? In this study, we used an event-related fMRI experiment to measure the fMRI response to paired stimuli moving in the same, orthogonal, or opposite direction of motion. We observed a release from fMRI adaptation in the orthogonal and opposite conditions relative to the same condition. This is consistent with the second stimulus exciting a fresh, unadapted subpopulation of orientation and direction-selective neurons. At the same time, we also observed a weaker response to the second stimulus as the adapter stimulus which may be due to either neuronal or vascular effects. A psychophysical study was conducted to

determine speed discrimination sensitivities in a paradigm similar to the fMRI experiment. Subjects were adapted to the same adapter stimulus as in the fMRI experiment and were performed a 2-AFC speed discrimination with test stimuli moving in the same, orthogonal, or opposite direction of motion. The sensitivities for orthogonal was the highest followed by opposite then same. These sensitivities correlated well with visual areas V2 and V4V. This study suggests that motion-specific fMRI adaptation in visual areas has both neuronal and vascular components.

# Chapter 2

# Differential transient MEG and fMRI responses to visual stimulation onset rate

## 2.1 Abstract

Nearly all methods for analyzing and interpreting functional magnetic resonance imaging (fMRI) data assume a linear relationship between the blood-oxygenated-level-dependent (BOLD) signal and the underlying neuronal response. While previous studies have shown that this 'neurovascular coupling' process is approximately linear, short stimulus durations are known to produce a larger fMRI response than expected from a linear system. This divergence from linearity between the stimulus time-course and BOLD signal could be caused by neuronal onset and offset transients, rather than a nonlinearity in the hemodynamics related to BOLD contrast. We tested this hypothesis by measuring MEG and fMRI responses to stimuli with ramped contrast onsets and offsets in place of abrupt transitions. MEG results show that the ramp successfully reduced the transient onset of neural activity. However, the nonlinearity in the fMRI response, while also reduced, remained. Predictions of fMRI responses from MEG signals show a weaker nonlinearity than observed in the actual fMRI data. These results suggest that the fMRI BOLD nonlinearity seen with short duration stimuli is not solely due to transient neuronal activity.

## 2.2 Introduction

Functional magnetic resonance imaging (fMRI) has grown as a powerful noninvasive tool for studying and detecting patterns of activation in the human brain. While there are many variants of fMRI, the most prevalent is blood-oxygenated-level-dependent (BOLD) fMRI. The BOLD signal is thought to reflect changes in deoxyhemoglobin content in local venous microvasculature (Bandettini et al. 1992; Belliveau et al. 1991; Kwong et al. 1992; Ogawa et al. 1992). These changes in deoxyhemoglobin concentration correlate with neuronal activity and are dependent on a complex interaction between cerebral metabolic rate of oxygen ($CMRO_2$), cerebral blood flow (CBF), and cerebral blood volume (CBV) (for review, see Heeger and Ress 2002).

A relationship is linear if it satisfies the properties of scaling and superposition (a weighted sum of input waveforms produces a weighted sum of individual output responses (Miller et al. 2001). Ideally, the transformation between neuronal activity and BOLD signal should be linear so that the fMRI response reflects the underlying neuronal response averaged over a small region of space and a short period of time. Although it is unlikely that the BOLD signal is truly a linear system due to the complexity of the neurovascular coupling process, even an approximation of linearity would greatly simplify the analysis and interpretation of the fMRI signal.

Nearly all fMRI data analysis methods assume a linear relationship between the BOLD signal and the underlying neuronal response. The assumption of linearity is supported by previous studies that show, to a first approximation, the fMRI response can be predicted by a linear convolution in time of the physical stimulus (Boynton et al. 1996; Dale and Buckner 1997; Glover 1999; Vazquez and Noll 1998). This means that the fMRI response to a long duration stimulus can be predicted by the fMRI response to a short duration stimulus. However, brief stimuli (lasting less than 3 or 4 seconds) have been shown to produce disproportionately large fMRI responses relative to longer duration stimuli in visual and auditory cortices (Boynton et al. 1996; Robson et al. 1998; Vazquez and Noll 1998). For example, 250 ms stimulus can produce an fMRI response that is 3-5 times larger than predicted from the response to a longer stimulus, and this nonlinearity can vary within and across cortical areas (Birn et al. 2001).

It is unclear whether this is due to a nonlinear neuronal response, a nonlinear hemodynamic response, or to a combination of both. Recent studies have shown evidence of a nonlinearity between CBF and BOLD and in particular, hemodynamic refractoriness has been suggested to explain why shorter duration stimuli have disproportionately larger responses (Mechelli et al. 2001; Miller et al. 2001; Obata et al. 2004). There is supporting evidence of this from fMRI and optical imaging experiments that show how the hemodynamic response to a stimulus is strongly affected by previous stimuli

(Cannestra et al. 1998; Dale and Buckner 1997; Friston 1998; Huettel and McCarthy 2000, 2001; Inan et al. 2004).

An alternative hypothesis is that the BOLD nonlinearity in visual (Boynton et al. 1996) and auditory (Robson et al. 1998) is caused by rapid neuronal adaptation, where a large burst of initial activity quickly decays to a weaker sustained response (Albrecht et al. 1984; Bonds 1991; Maddess et al. 1988). Electrophysiological data has shown large transients in the neuronal response at the stimulus onset and offset (Albrecht et al. 1984; Muller et al. 2001, 1999). Since these transients presumably occur equally for stimuli of all durations, they should have a disproportionately larger influence on the average response for shorter stimulus durations than for longer stimulus durations. This could explain the larger relative BOLD signal to stimuli that last less then 4 seconds. Neuroimaging studies suggest that neuronal onset transients may be the source of identifiable BOLD onset transients that may be used to characterize schizophrenia (Fox et al. 2005a; Fox et al. 2005b).

The goal of the present study was to test the degree to which transients in the neuronal response can account for the observed BOLD nonlinearity. This was accomplished by smoothing the temporal profile of visual stimulation by introducing a slow contrast ramp at the onset and offset of the visual stimulus. To confirm that the ramped stimulus successfully reduces the transient overshoot, we first took advantage of the high temporal resolution of

magnetoencephalography (MEG) to observe the response in visual cortex to our ramped and un-ramped stimuli.

Using the MEG response as a surrogate for neuronal activity, we predicted an fMRI response to the ramped stimuli. We then examined the linearity between the stimulus and the MEG-derived fMRI predictions and the linearity between the stimulus and the measured BOLD responses. While nonlinear dynamical systems may be used to characterize nonlinearities (Friston 2002; Friston et al. 2000), we approach this question from a linear-systems standpoint. The MEG-derived fMRI predictions show a nonlinearity associated with short stimulus durations, but this nonlinearity is much smaller than the observed nonlinearity in the BOLD signal. We therefore conclude that the BOLD nonlinearity is not solely due to transient onset activity.

## 2.3 Materials and methods

### 2.3.1 Subjects

Thirteen subjects underwent a complete physical examination and provided informed consent (fMRI experiment, N = 10; MEG experiment, N = 5; two subjects participated in both experiments). All subjects had normal or corrected-to-normal visual acuity. All subjects were free of neurological or psychiatric illness and were compensated for participation in the study, and anatomical MR scans were screened by the NIH Clinical Center Department of

Radiology in accordance with the National Institute of Mental Health Institutional Review Board guidelines.

### 2.3.2 MEG stimulus presentation apparatus

Stimuli for the MEG experiments were generated on an Apple PowerMac G3 laptop computer (Apple Computers, Cupertino, CA) using Matlab version 5.2 (MathWorks, Natick, MA) and the Psychophysics Toolbox (Brainard 1997; Pelli 1997). Stimuli for the MEG experiments were produced using a Sharp PG-210U projector (Camus, WA) fitted with a zoom lens, located outside of the scanner room, and passed the images through a guide tube. During MEG data acquisition, subjects were placed in a seated position and directly viewed the image on a back-projection screen located 74 cm in front of the subject. Subjects' heads were stabilized with an airbladder and chinstrap system.

### 2.3.3 MEG stimulus

In both our MEG and fMRI experiments, the stimulus consisted of a full-field (12° vertical by 15° horizontal) counterphase flickering checkerboard at 8 Hz. A square fixation point was placed in the center of the visual field, and a uniform gray field of the same mean luminance as the checkerboard with a central square fixation point was presented between stimulus presentations. Stimuli had either an abrupt onset and offset (the no-ramp condition), or had onsets and offsets in which the contrast over time followed a raised cosine

function (figure 2.1). The definition of stimulus duration for these ramped conditions is the time between 50% of the maximum contrast. Stimuli had durations of either 1 or 2 seconds, and had ramp durations of 0, 0.5 or 1 second in length. Since eyeblink frequency is variable (Doughty 2001), subjects were allowed to blink at their own comfortable frequency. However, even with online and offline correction, subject eyeblinks create very large artifacts in MEG data. Short stimulus durations were thus chosen to avoid eye blink artifacts from intruding during the stimulus presentation. To maximize the amount of data collected during a run, the inter-stimulus interval (ISI) was 3 seconds and defined as the duration between the 50% of the maximum contrast between stimulus presentations. Ramp and stimulus durations were constant within each acquired 242-second run that was divided into 4 or 5 second epochs. Subjects fixated on a square fixation point placed in the center of the visual field without a task. An MEG session consisted of 6 runs to examine each combination of the two stimulus durations and three ramp conditions.

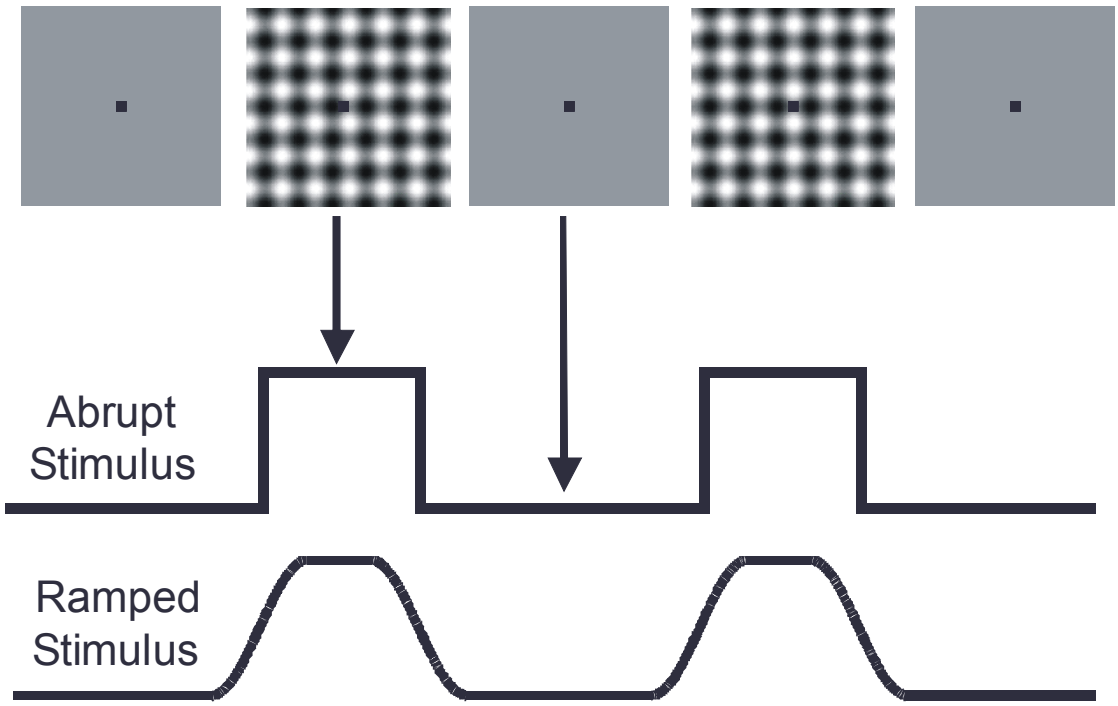


Figure 2.1: Ramped Paradigm Design. Abrupt on/off transitions were substituted with a ramped transition modeled after a raised cosine function. Gray background presentations were fixed (3 seconds for MEG and 15 seconds for fMRI) while checkerboard stimulus presentations varied (1 or 2 seconds for MEG and 1, 3, 6, or 12 seconds for fMRI). Inter-stimulus interval durations were defined as the duration between 50% of maximum contrast between stimulus presentations. Stimulus duration was defined as the duration between 50% of maximum contrast.

### 2.3.4 MEG data acquisition

During each run, MEG data was collected on five subjects in a 275-channel CTF scanner (Coquitlam, British Columbia, Canada) at a sampling rate of 600 Hz.

### 2.3.5 MEG data analysis

Noise from the acquired MEG data was removed with a 3$^{rd}$ order gradient. The DC offset and 60 Hz powerline were also subtracted. Data was high passed filtered at 0.7 Hz. 500 ms of data around eye blinks (exceeding 1pT in amplitude and 1pT/second) were computationally identified and removed. The stimulus epochs were then averaged within each acquisition for each channel. The amplitude of the MEG response was converted into the frequency domain by computing the Stockwell transform, from the averaged acquisitions. The Stockwell transform is similar to the Fourier transform with the primary difference that frequency-dependent Gaussian time windows are utilized (Goodyear et al. 2004). This creates a tradeoff between increased temporal resolution at higher frequencies where narrower time windows are used and increased frequency resolution at lower frequencies where wider time windows are used. Evoked rather than induced responses were investigated because the detection of induced responses requires a signal to noise ratio that is at least two orders of magnitude greater than that of evoked responses (Lin et al. 2004). Also a recent MEG study investigating temporal frequency tuning in visual cortex found robust effects in evoked responses and

weak responses in induced or non phase-locked responses (Fawcett et al. 2004). The evoked responses were interpreted to reflect the steady state visual evoked potential and represent direct driving of neurons in primary visual cortex (Fawcett et al. 2004).

A counterphase-modulated stimulus typically induces a frequency-doubled MEG and EEG signal (Fawcett et al. 2004). As an additional analysis restricted to this frequency range, we applied a wavelet convolution with a 16Hz kernel to the averaged MEG response. This convolution provides a measure of the power of the MEG signal at the frequency we expect the stimulus response to occur.

### 2.3.6 fMRI stimulus presentation apparatus

Stimuli for the fMRI experiments were generated with the same system and stimulation program used in the MEG experiments. Images were produced using a Sharp PG-210U projector (Camus, WA) fitted with a zoom lens and projected onto a back projection screen. Viewing distance was 367 cm. Projector refresh rate was 60 Hz. During fMRI data acquisition, subjects viewed the image on a screen near the subject's legs through a mirror mounted to the MRI table above the subject's eyes. Subjects' heads were stabilized with a vacuum-pack pillow system (S&S Technology, Houston, TX) system.

### 2.3.7 fMRI stimulus

Stimulus durations were 1, 3, 6, or 12 seconds and ramp durations were 0, 0.5, and 1 second in length. These stimulus durations were chosen to duplicate previous findings (Boynton et al. 1996) and to overlap with at least one of the stimulus durations presented in the MEG stimulus paradigm (i.e. the 1 second stimulus duration). The ISI was 15 seconds to allow for a recovery of the hemodynamic response (Boynton et al. 1996). Using a shorter ISI would potentially change the fMRI response to subsequent stimuli (Dale and Buckner 1997; Huettel and McCarthy 2000). Each fMRI scan lasted 242 seconds with ramp and stimulus durations held constant. Each experimental session consisted of 12 stimulus scans (one for each combination of stimulus and ramp duration) followed by an anatomical scan (MPRAGE; 1x1x1 mm resolution), using a standard T1-weighted gradient echo pulse sequence. The stimulus scans were presented in random order. During the fMRI scans, subjects fixated on the square fixation point and performed a one-back task comparing stimulus duration.

### 2.3.8 fMRI data acquisition

A series of 242 axial T2*-weighted echo planar images (EPI) was acquired on a 3-T GE Signa MR scanner (Waukesha, WI, USA) (TR: 1 s; TE: 30 ms; field of view: 24 cm; slice thickness: 5 mm; 90° flip angle; matrix size: 64 x 64). A brain-specific quadrature Medical Advances RF coil was used (Wauwautosa, WI, USA). A limited coverage of 8–12 slices was used, allowing

a TR of 1 s in order to improve sampling of the hemodynamic response. An additional set of high resolution, T1-weighted, inversion-recovery spoiled gradient-echo anatomic reference images (TE = 5.3 ms, TR = 12 ms, TI = 725 ms, FOV = 24 cm, matrix = 256 × 192, slice thickness = 1.2 mm, 17° flip angle, and 124 axial slices) were obtained for localization purposes.

### 2.3.9 fMRI data analysis

Data were analyzed by fitting the ideal hemodynamic BOLD response to each pixel's entire signal intensity time course. These ideal time responses were computed by convolving a gamma variate function $h(t) = t^{8.6}\ e^{-t/0.547}$ (Cohen 1997) with stimulus blocks consisting of boxcars of the nominal stimulus duration. This multiple linear regression analysis was performed using Analysis of Functional NeuroImages (AFNI) software, including a regressor to model linear trends, or drifts, in the data (Cox 1996). Only voxels in visual cortex exceeding a correlation threshold of 0.3 for all combinations of stimulus and ramp duration within a subject were used to define the subject's region of interest (ROI). A voxel which did not exceed this threshold for every combination was excluded from the ROI. While there is spatial heterogeneity of BOLD responses within an ROI (Birn et al. 2001; Pfeuffer et al. 2003), we utilized a relatively large ROI for our fMRI analyses to mirror the large ROI used in our MEG analyses. The majority of fMRI studies are also concerned with the BOLD responses from ROIs rather than single-voxel response profiles. Time courses of voxels in each subject's ROI were averaged for each

combination of stimulus and ramp condition. These averaged response time courses were used in a linear systems analysis similar to (Boynton et al. 1996) to test the effects of varying ramp and stimulus durations. In this analysis, the hemodynamic responses to long duration stimuli were predicted by summing copies of appropriately shifted responses to short duration stimuli. The four stimulus durations of 1, 3, 6, and 12 seconds provide 6 predictions. For example, shifting and adding four responses to a 3-second stimulus was used to predict the response to a 12-second stimulus.

### 2.3.10 Prediction of fMRI response from MEG data

MEG response curves for each stimulus and ramp duration were generated by summing the amplitudes of the Stockwell Transformation in the 0-40 Hz range. Estimates of the MEG response to longer stimulus durations of 3s, 6s, and 12s were obtained by extending the steady-state period (filling in a value equal to the average amplitude during this steady state), and using for the ramp periods an average of the response during the ramps from the 1s and 2s stimuli. Each of these MEG response curves was convolved with a gamma-variate function to represent an ideal hemodynamic BOLD response. These convolved predictions were compared with the fMRI data.

The degree of nonlinearity for both the measured BOLD response and the MEG predicted BOLD response was computed by fitting ideal response functions (a gamma variate convolved with a boxcar of width equal to the nominal stimulus duration). These fit values were scaled by the amplitude of

the fit to the longest (12s) duration response. If the relationship between the stimulus and the MEG response was linear, then the fit values of these ideal responses should be the same for all stimulus durations, and the degree of nonlinearity should be equal to 1. Finally, the linearity of the MEG-predicted BOLD response was also assessed by superposition, in order to allow a direct comparison with the analysis performed for the fMRI study. This comparison can show how much of the nonlinearity revealed for the BOLD response can be explained by the neuronal transients, as measured with MEG.

## 2.4 Results

### 2.4.1 MEG experiment

We first examined the ramp paradigm with MEG because it offers the high temporal resolution necessary to determine if a ramped onset reduces the transient response. A counterphase-modulated stimulus induces a frequency-doubled MEG and EEG signal. This can be seen in the Stockwell transformation (figure 2.2), which shows a strong 16Hz response to the 8Hz stimulus. Figure 2.2 shows the average of the Stockwell transformed MEG responses averaged across all occipital channels. As expected, the predominant response for each ramp and stimulus duration occurs at 16 Hz. Robust transient responses near the onset of the stimuli in the no-ramp condition are evident for both stimulus durations of 1 and 2 seconds (figure 2.2 A and D). This is in agreement with a previous MEG study showing transient onset response in the 5 – 10 Hz range (Fawcett et al. 2004). In the 0.5 and 1

second ramp condition (figure 2.2 B-C, D-E), the transient response is reduced regardless of stimulus duration. The longer ramp duration shows the greatest reduction in transient response. The steady state response to the stimulus appears to be the same across all ramp durations.

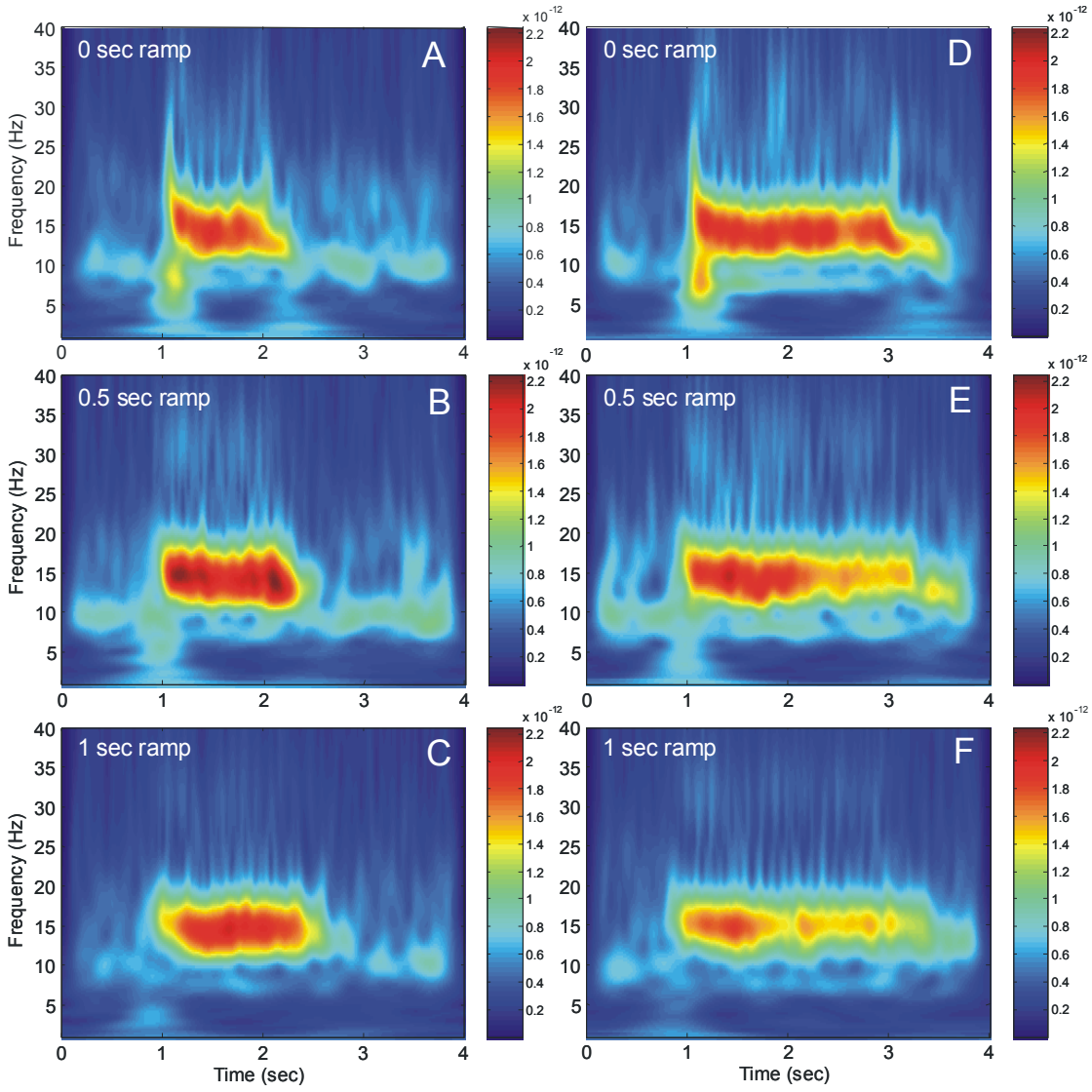


Figure 2.2: Stockwell Transformation of MEG responses. Time-frequency plots created using a Stockwell transformation on our averaged MEG recordings in occipital sensors. The time window decreases with frequency. The left column (A-C) shows responses to a stimulus of 1 second in duration while the right column (D-F) shows the response to a 2 second stimulus. A transient onset response in the 5-30 Hz range can be seen at stimulus onset in the no-ramp condition while a reduction of the transient onset response is observed in the 1 second ramp condition. The 0.5 second ramp condition shows a moderate reduction in transient onset response. The color bar to the right of each figure shows the amplitude of the response.

Figure 2.3 shows the summed amplitude of the Stockwell transformation in the 0-40 Hz range. For both 1 and 2-second stimulus durations, the summed amplitudes show robust transient onset responses for the no-ramp condition and a reduction in transient response in the 1 second ramp stimulus. The MEG response to a 1-second ramped stimulus shows a rapid increase during the ramp, reaching steady state levels after only a relatively small change in contrast. Steady state responses are similar in all four conditions. This produces a similar pattern of transient response attenuation as seen in the Stockwell transformations and suggests that the ramped stimulus paradigm reduces the transient onset response across all frequencies as measured by MEG. These findings demonstrate that varying the duration of a ramped onset and offset may modulate and attenuate the transient MEG response.

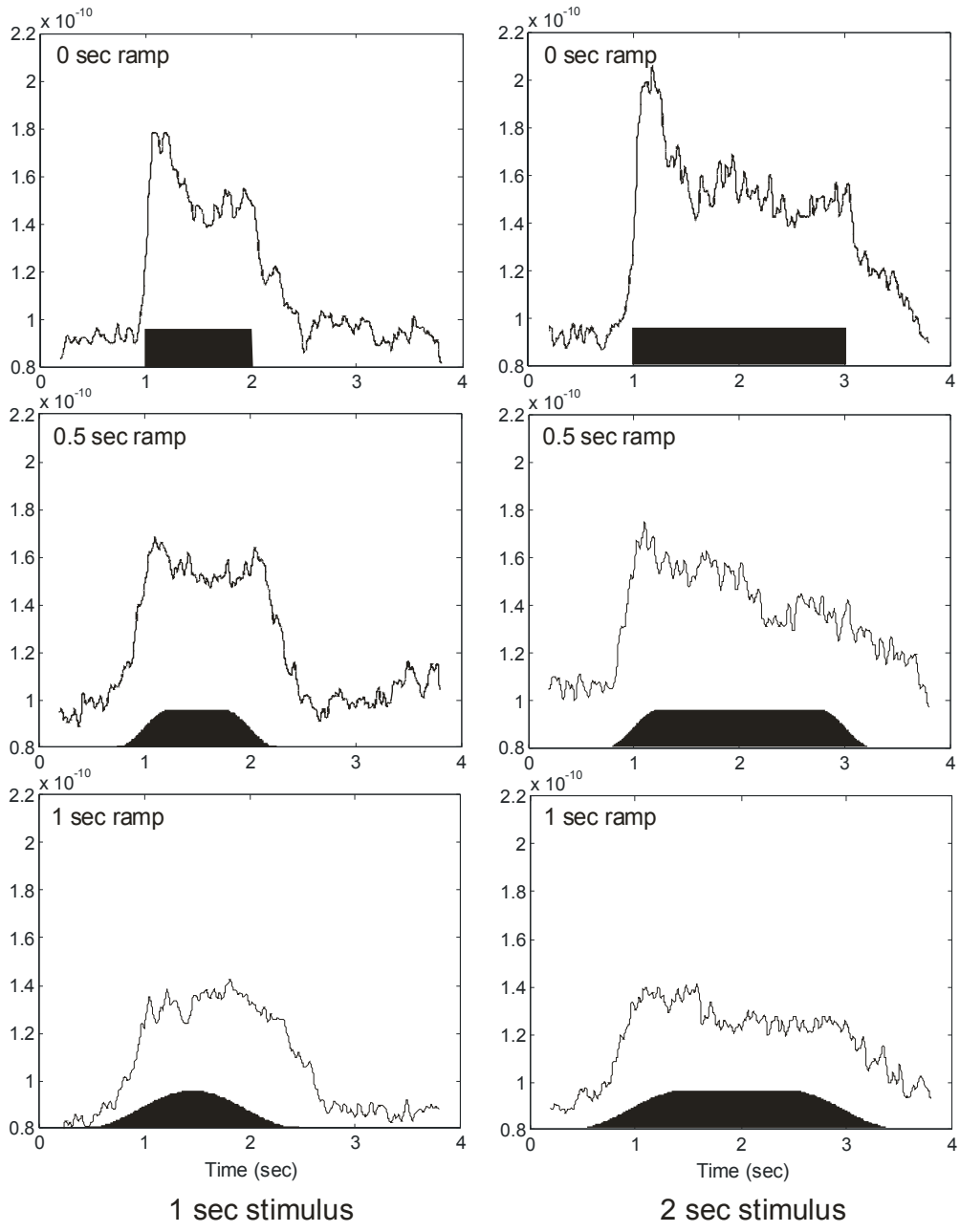


Figure 2.3: Summed amplitudes of the Stockwell Transform. The amplitudes in the 0-40 Hz range from the Stockwell Transformation in figure 2.2 are summed. Below each summed response is the maximum stimulus contrast as a function of time. The left column shows responses to a stimulus of 1 second in duration while the right column shows the response to a 2 second stimulus. A transient onset response can be seen at stimulus onset in the no-ramp condition while a reduction of the transient onset response is observed with increasing ramp duration.

### 2.4.2 fMRI experiment

We tested the ramp paradigm's effect on the linearity of the fMRI response by examining whether responses to long duration stimuli could be predicted by short duration stimuli (Boynton et al. 1996). Figure 2.4 shows the results of the predictions in the no-ramp condition. The shifted copies of the response to the shorter duration stimulus are shown with solid lines, the response to the longer duration stimulus is shown with the long dashed line, and the prediction is shown with the short dashed line. This replicates the original examination of linearity in fMRI (Boynton et al. 1996) but with additional shorter duration stimuli and with Vazquez and Noll's work where they demonstrated increasing nonlinear behavior with short duration stimuli when using a sinusoidally ramped onset and offset. Consistent with previous studies (Boynton et al. 1996; Vazquez and Noll 1998), the fMRI response is approximately linear when the 6-second stimulus is used to predict the 12-second response, but diverges from linearity when predicting with short stimulus durations (1 and 3 seconds). The overprediction becomes increasingly exaggerated when predicting longer stimulus durations.

Figures 2.5 and 2.6 show the same analysis for the 0.5 and 1-second ramp conditions, respectively. The predictions of the fMRI responses in these conditions are remarkably similar to the no-ramp condition, showing a disproportionately large response with shorter duration stimuli with a tendency towards a linear approximation of the fMRI response signal with longer

duration stimuli. This trend is consistent for all six comparisons. The similarity of the fMRI results across ramp durations is quite striking in light of how increasing the ramp duration attenuates the MEG transient response. In contrast to our MEG results, presenting a ramped stimulus instead of an abrupt onset and offset stimulus does not change the nonlinearity of the fMRI response. Increasing the duration of the ramp also does not modulate the nonlinearity of the fMRI response.

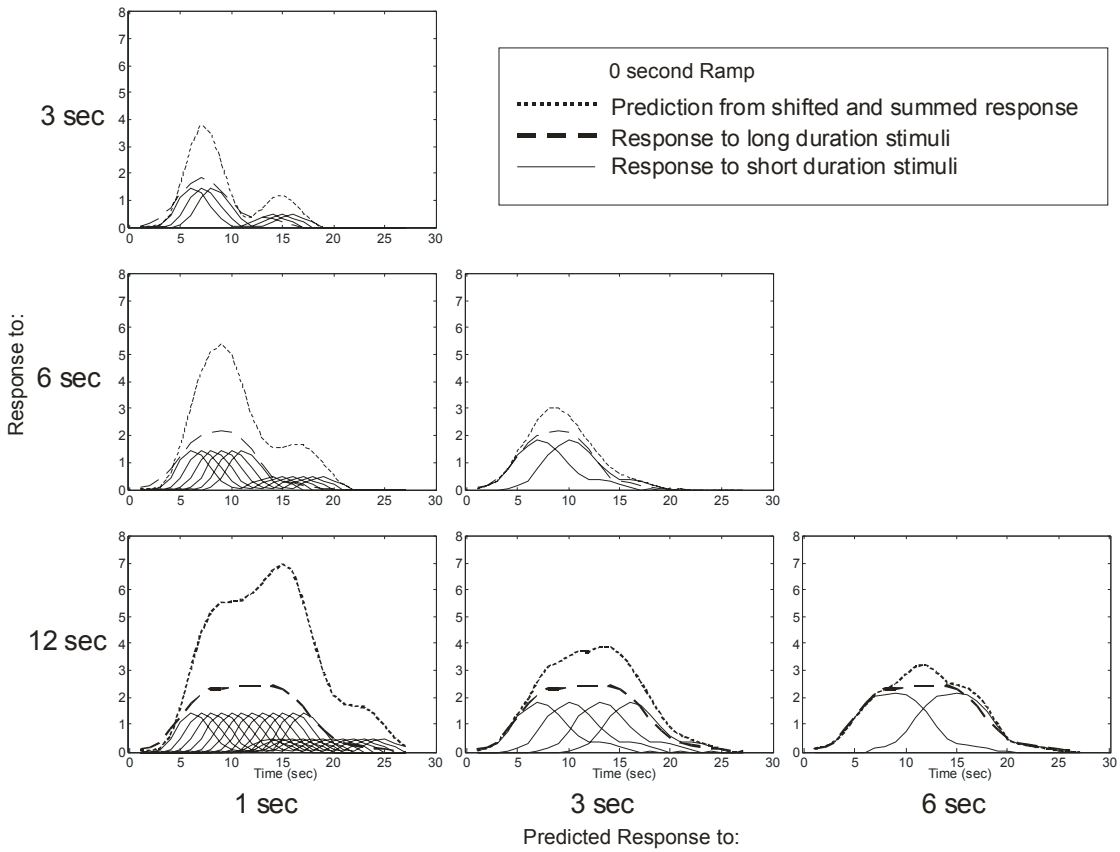


Figure 2.4: Tests of Superposition, 0 second Ramp Stimulus. Responses to longer duration stimuli (long dashes) are predicted by superposition of responses to shorter duration stimuli (short dashes). The shifted copies of the response to the shorter duration stimuli are shown in solid lines. These predictions used stimuli with no ramped onset. fMRI responses to 1, 3, and 6 seconds were used to predict the response to 3, 6, and 12 seconds. The system becomes more linear with longer durations, but a large non-linearity occurs with short duration stimuli (1 second).

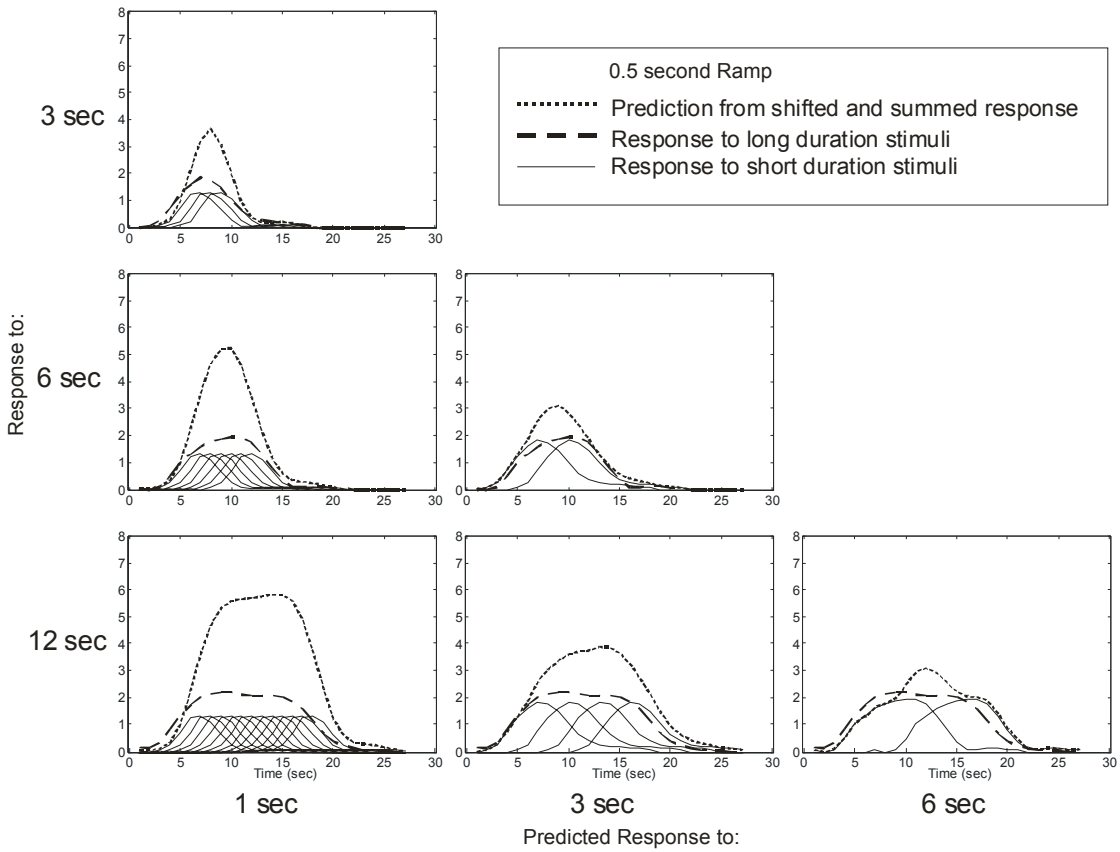


Figure 2.5: Tests of Superposition, 0.5 second Ramp Stimulus. These predictions used stimuli with a 0.5 second ramped onset. fMRI responses to 1, 3, and 6 seconds were used to predict the response to 3, 6, and 12 seconds. As in the no ramp condition, the system becomes more linear with longer durations, but a large non-linearity occurs with short duration stimuli (1 second). Utilizing a 0.5 second ramp does not appreciably reduce the non-linearity at short durations.

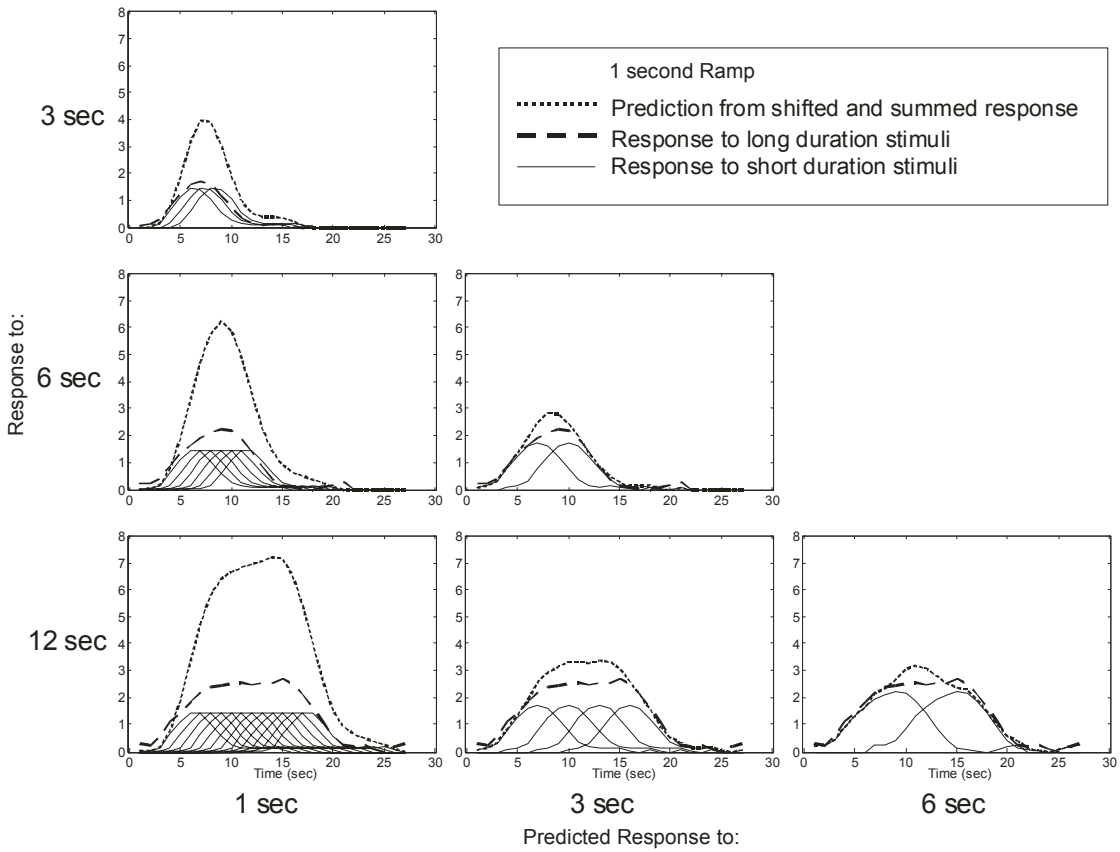


Figure 2.6: Tests of Superposition, 1 second Ramp Stimulus. These predictions used stimuli with a 1 second ramped onset. fMRI responses to 1, 3, and 6 seconds were used to predict the response to 3, 6, and 12 seconds. As in the no ramp and 0.5 second ramp conditions, the system becomes more linear with longer durations, but a large non-linearity occurs with short duration stimuli (1 second). Utilizing a 1 second ramp also does not appreciably reduce the non-linearity at short durations.

### 2.4.3 A different definition of ramp duration

The precise duration of a ramped stimulus depends on its definition. In this study, the duration of the stimulus was defined as the time between 50% contrast because with raised cosine ramps, the superposition analysis is valid with respect to the physical stimulus. For example, three shifted copies of a 1-second ramped stimulus will add perfectly to form a single 3-second stimulus.

However, as known from earlier studies and evident from our MEG data, the neuronal response is not necessarily a linear function of contrast; neuronal and fMRI responses at lower contrasts are disproportionately larger than at higher contrasts (Boynton et al. 1999; Boynton et al. 1996; Logothetis et al. 2001). So while the ramp may reduce the transient overshoot activity relative to the steady state, it may also effectively increase the duration of the neuronal response. Our initial test for superposition may therefore not yield a fair prediction because although the physical stimuli may shift and add appropriately, the neuronal responses may not.

We therefore conducted a second test of superposition by assuming the extreme case of defining the stimulus duration to include the entire ramp duration (figure 2.7). That is, a 1-second stimulus with a 0.5 second ramp duration was considered to have a duration of 1.5 seconds, so that only two shifted copies of the response were used to predict a 3-second stimulus. Superposition in this extreme case means that the neuronal response is firing at its steady-state level for the duration of the stimulus, including the ramp.

This analysis should skew the prediction to underestimate the response to the longer stimulus duration.

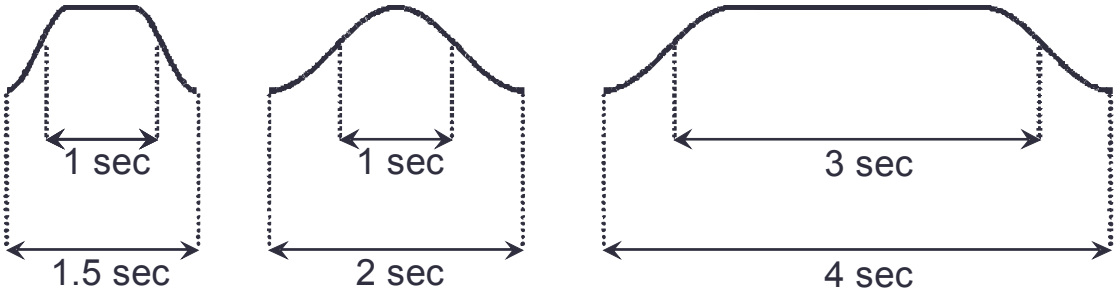


Figure 2.7: Alternate definition of stimulus duration. The initial definition of stimulus duration was the width of the stimulus at half-maximum of its contrast (shown in the top set of arrows). The alternative, or "strict," definition of stimulus duration includes the entirety of the ramp onset and offset durations (shown in the bottom set of arrows).

Figure 2.8 shows the results of the predictions when utilizing this new definition of stimulus duration. Only comparisons between conditions which shared the same ramp condition and whose longer stimulus duration was a multiple of the shorter stimulus duration were examined. Even with this extreme definition of stimulus duration, we still see an overprediction of the response to longer stimuli from shorter stimulus durations. That is, even though we are now summing fewer responses to generate the predicted response, we still observe a disproportionately large fMRI response to short duration stimuli. This overprediction from short stimulus durations, after accounting for a possible lengthening of the response, is strong evidence that our fMRI response to the stimulus remains nonlinear with the ramp.

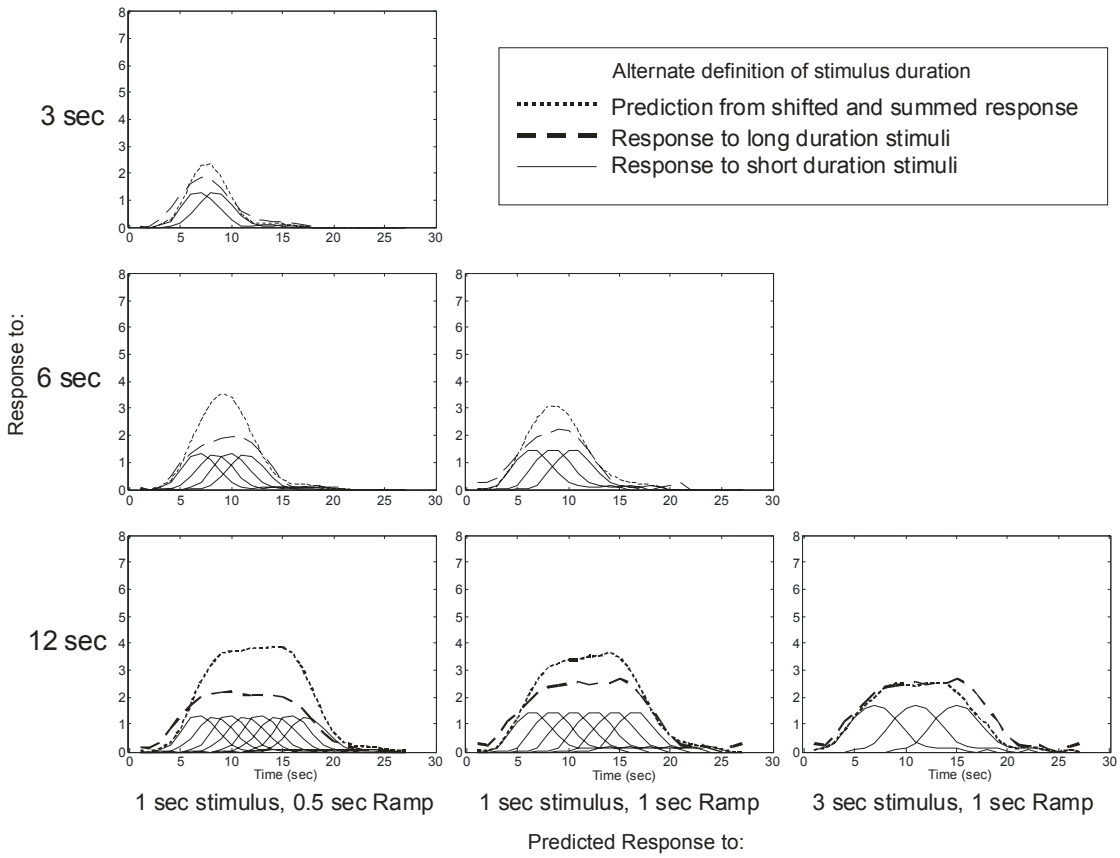


Figure 2.8: Test of superposition using an alternative definition of stimulus duration. Using a more conservative yet skewed interpretation of stimulus duration still generates an overprediction at short duration stimuli. Stimulus duration includes the ramp durations and is defined as the duration from stimulus onset to offset. In all cases except for one, a longer response (3, 6, or 12 seconds) was predicted by the fMRI response to a 1 second stimulus duration (as defined by the old definition) with the same ramp duration as the longer response. In the bottom right figure, the comparison is with a 3 second stimulus duration and 1 second ramp predicting the response to a 12 second stimulus with the same ramp duration.

### 2.4.4 Predicting the fMRI response from MEG data:

Another way to compare the results across methodologies is to directly predict the fMRI response from the MEG response by convolving the total MEG output in the 0-40 Hz range with a hemodynamic impulse response function. Each combination of stimulus and ramp duration was convolved separately. Figure 2.9 shows the actual and predicted fMRI response to different ramp and stimulus durations. Qualitatively, the MEG-derived fMRI response does not appear to show the large nonlinearity at shorter stimulus durations that exists in the fMRI data. Figure 2.10 (A and B) shows the regression analysis of fitting the ideal responses (based on a simple boxcar stimulus convolved with a gamma-variate function) to the data. With longer stimulus durations, the fits approach unity with both the BOLD data and the MEG-derived BOLD predictions, but with the shortest stimulus duration (1 second), there is a deviation from unity. The BOLD data at 1 second shows a nonlinearity of approximately 2.5-fold relative to the ideal fit while the MEG-derived prediction has a nonlinearity of approximately 1.5-fold. The slight nonlinearity of the MEG response to the stimulus is due to an overshoot in the neuronal activity relative to the steady state for the 0s and 0.5s ramp durations, and to an increased duration of the neuronal response (relative to the nominal stimulus duration) for the 0.5s and 1s ramp durations. While the MEG-derived BOLD prediction demonstrates a disproportionately large

increase at short stimulus durations, it is dwarfed by the BOLD response's nonlinearity.

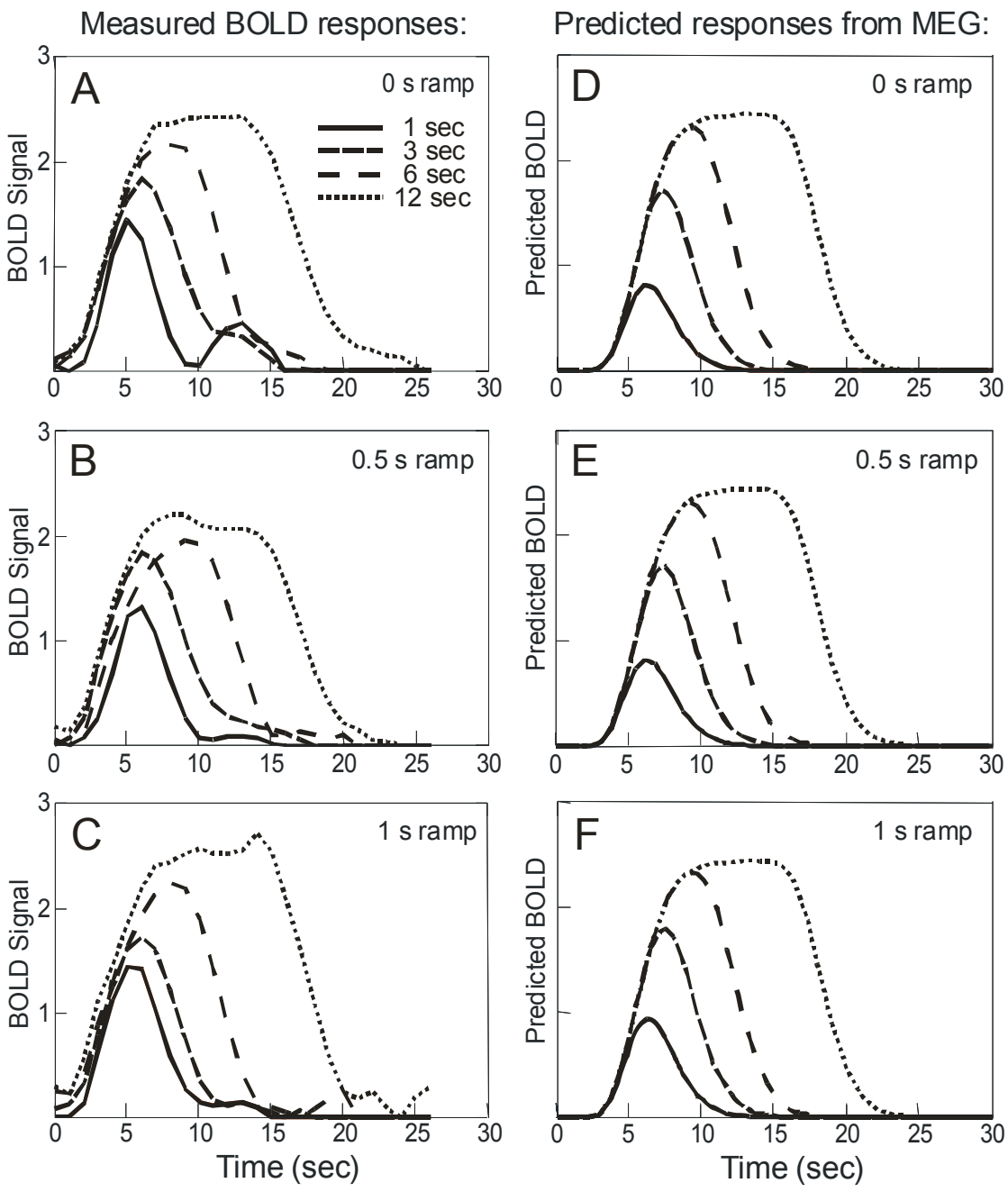


Figure 2.9: Predicting fMRI responses from MEG Data. Time courses of fMRI signal to different stimulus durations and ramp durations (A-C). Predicted fMRI responses to the same conditions using MEG signal (D-F). The MEG responses are convolved with a hemodynamic response filter to generate the predicted responses. fMRI responses to longer duration were generated by extending the steady-state MEG response to shorter durations then convolving with the hemodynamic response filter.

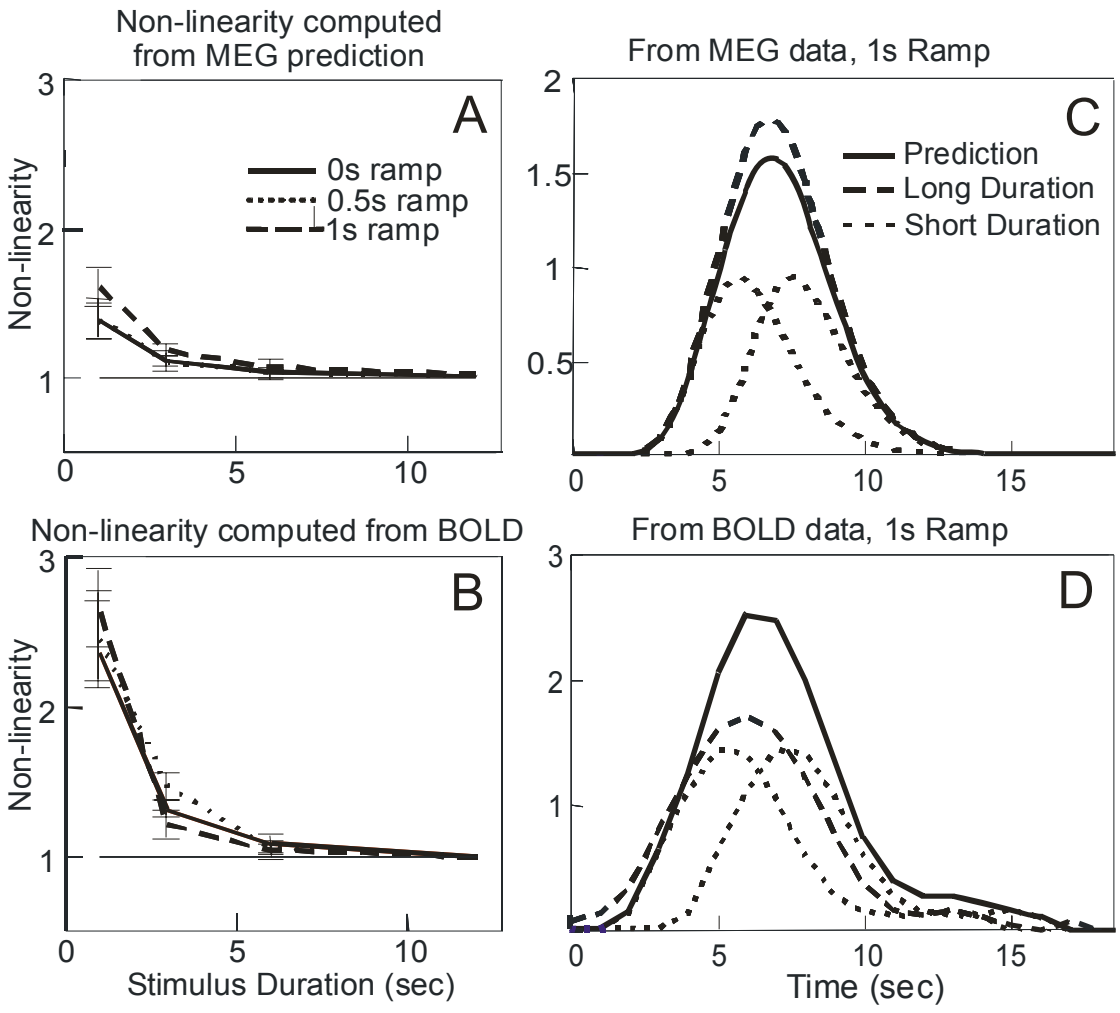


Figure 2.10: Nonlinearity in MEG-derived and BOLD responses. Fitting the actual and predicted fMRI time courses to an ideal response shows a deviation from linearity with short stimulus durations. While we observe an over response in the MEG-derived predicted time courses (A), we see a larger nonlinearity in the BOLD time courses (B). Assuming the alternative definition of stimulus duration, we observe the predicted response (solid line) from shorter responses is smaller than the response to the long duration stimulus (long dashed line) in the MEG-derived time series (C). However, using this alternative definition, the predicted response (solid line) is much larger than the response to the long duration stimulus (long dashed line) in the BOLD time courses (D).

Since the MEG response to the 1s and 2s stimulus durations with a 1s ramp appeared similar to boxcar functions of 2s and 4s durations, respectively, the linearity was also assessed by summing two copies of the MEG-predicted BOLD response to a 1s stimulus and comparing this to the MEG-predicted BOLD response for a 3s duration stimulus (figure 2.10). This is analogous to the "extreme" case shown in figure 2.8, which as discussed earlier clearly illustrates the continued overprediction even when fewer responses are summed to create the predicted response. In this case, however, the MEG-derived fMRI responses show an underprediction of the longer stimulus duration when using a different definition of the stimulus duration. The convolved response to a stimulus of 3 seconds in length is larger than the summed and shifted responses to two stimuli that are 1 second in length. This again demonstrates that the nonlinearity measured in BOLD responses is much larger than would be predicted based on MEG responses.

## 2.5 Discussion

The fMRI response has been shown to be disproportionately large for short stimulus durations (Boynton et al. 1996; Dale and Buckner 1997; Vazquez and Noll 1998). This nonlinearity has been shown to vary considerably across space with a given voxel showing an 8-fold over-prediction while a nearby voxel had only a 3-fold nonlinearity (Birn et al. 2001). While one group has explored the possibility of hemodynamic transients through simulations (Obata et al. 2004), no previous study has directly

examined the degree to which transients in the neuronal response can account for the observed BOLD nonlinearity, and how the nonlinearity is affected when these transients are modulated.

In the first part of our study, we took advantage of the high temporal resolution of MEG and found that the MEG transient onset and offset response is reduced with the presentation of a ramped onset and offset instead of an abrupt transition in contrast. We also observed that the transient response as measured with MEG is reduced with increasing ramp durations. However, our fMRI responses to the ramped paradigm showed no change in the nonlinearity of the fMRI signal to short duration stimuli. Modulating the duration of the ramped onset and offset also did not influence the amount of nonlinearity in the fMRI signal, with responses to the 1-second stimuli showing a 2.5-fold over-prediction. In comparison, using the MEG responses as surrogates for neuronal responses, the 1 second stimulus shows only a 1.4-fold over-prediction. This means that the amount of the nonlinearity that can be explained by the neuronal transients measured by MEG is not sufficient to account for all of the nonlinearity in the BOLD response, explaining only about half of the observed overshoot. These results suggest that the fMRI nonlinearity in the fMRI response is not solely due to the transient neuronal activity. The source of this additional nonlinearity must therefore either be hemodynamic in origin or the result of other neuronal effects not accounted for in the MEG measurement.

One possible vascular explanation is that a minimal increase in neuronal activity could lead to a dramatic increase in blood flow. Logothetis (2001) showed that local field potentials (LFP) and multi-unit activity (MUA) increased with stimulus contrast at a slower rate then the fMRI response. They demonstrated that at 12.5% contrast, the steady-state fMRI response was already at 50% of maximum amplitude while LFP and MUA activity was only about 20% of maximum. There therefore appears to be a relatively large BOLD signal associated with a small amount of neuronal activity.

The larger than expected responses to brief stimuli may also be the result of a nonlinear relation between the oxygen extraction fraction and cerebral blood flow. A recent work examining the BOLD response to different stimulus duty cycles and stimulus "off" periods has shown that only about half of the observed nonlinearity could be predicted from nonlinearities in the hemodynamic response (Birn and Bandettini 2005).

The spatial heterogeneity of the regions of interest (ROIs) used in our MEG and BOLD analysis may also have an influence in the comparison of our two results. In fMRI, the amount of non-linearity has been shown to be spatially dependent, with some areas of the visual cortex being more non-linear than others (Birn et al. 2001). fMRI ROIs were restricted to voxels responding to stimuli in all conditions, whereas in MEG, the "ROI" consisted of all the occipital sensors. Although both analyses presumably reflect a

population response, the ROIs in the two methods may reflect responses in different spatial locations.

An additional reason for the difference in the nonlinearity predicted by MEG and observed in BOLD is that the MEG signal may not capture all of the neuronal activity in the cortex. The magnetic fields generated by the synchronous activity of pyramidal cortical neurons oriented perpendicular to the surface of scalp, for example, are generally not detected with MEG. However, in order to explain a change in the linearity, i.e. a change in the ratio of the transient to steady-state response, disproportionately more neurons that respond transiently to the stimulus must be undetected. This would only be possible if neurons which convey transient information during the ramp phase of the stimulus lie in an orientation perpendicular to the surface of the scalp, and are therefore undetected, while neurons responding to the steady-state response lie in an orientation more parallel to the scalp. In this case, one could use EEG to determine the existence of this population of perpendicularly-oriented neurons. The scenario of transient neurons lying in pooled groups of different orientations for different ramp durations seems highly unlikely. A decreased ability to detect neuronal activity by MEG can also result from a reduction in phase coherence among neurons. In this case, the magnetic fields sum incoherently and cancel each other, resulting in a decreased MEG response but with possibly no change in the neuronal metabolism and associated BOLD fMRI response. In order to explain a change in the linearity,

a greater phase incoherence coupled with increased metabolism must be present for brief stimuli and during the ramps in stimulus contrast.

### 2.6 Conclusion

In summary, our MEG measurements show that the abrupt onset of a visual stimulus induces a transient overshoot in neuronal activity. These transients are consistent with the way fMRI responses to shorter stimulus durations are larger than expected from a linear convolution of the stimulus time-course. Indeed, BOLD signals predicted from our MEG responses to abrupt onset stimuli do show disproportionately large responses to short stimulus durations, but this predicted nonlinearity is not as large as that observed in our fMRI measurements. The transient in the MEG signal is reduced when the contrast is ramped up slowly. This reduces the predicted nonlinearity in the BOLD signal. However, the BOLD response to short duration ramped stimuli remains disproportionately large.

Since the steady-state neuronal response is a decelerating function of stimulus contrast, our ramped stimulus effectively lengthens the duration of the neuronal response. If the contrast-response curve is taken into account by assuming a longer duration neuronal response, then the MEG response for a 1s ramp behaves more linear, while the BOLD response remains nonlinear. The neuronal overshoot with abrupt onset stimuli measured by MEG can only explain about half of the nonlinearity observed in the BOLD response. These results suggest that the nonlinearity of the fMRI response is not solely due to

transient activity, and that approximately half of it must be accounted for by other neuronal or vascular contributions.

**2.7 Acknowledgements**:

Fred Carver and Tom Holroyd for their assistance in MEG data acquisition and analysis.

The text of Chapter Two is a reprint of a manuscript submitted for publication of which I am the primary author. It has been submitted as August S. Tuan, Rasmus M. Birn, Peter A. Bandettini, and Geoffrey M. Boynton. “Differential transient MEG and fMRI responses to visual stimulation onset rate.” *Neuroimage*. 2006.

# Chapter 3

# fMRI Adaptation to Motion in Human Visual Areas is reflected in Behavioral Performance

## 3.1 Abstract

The fMRI adaptation paradigm has been used to study the contributions of specific subpopulations of neurons with voxels in both higher and lower visual areas. A number of studies have reported robust results using this technique although there has been little validation of fMRI adaptation using stimulus manipulations on well-known dimensions (such as direction of motion) in well-studied visual areas. The relative contributions of neuronal and vascular effects have also not been well characterized. We used an event-related fMRI experiment to measure the response to pairs of stimuli moving in the same, orthogonal, and opposite direction of motion in visual areas V1, V2, V3, V3A, V4V, and MT+. We observed weaker response to the second stimulus as compared to the first stimulus suggesting neuronal or vascular adaptation. We also observed a release from adaptation in the orthogonal and opposite conditions, which is consistent with the second stimulus accessing a fresh, unadapted subpopulation of neurons. Perceptual sensitivity in a speed discrimination task using the same moving stimuli as adapters correlate well with fMRI responses in visual areas V2 and V4V. These results

suggest that motion-specific fMRI adaptation in visual areas has both neuronal and vascular components.

### 3.2 Introduction

The fMRI adaptation paradigm has been used by a number of studies to reveal selective neuronal subpopulations at resolutions finer than in typical fMRI voxels (Engel 2005; Engel and Furmanski 2001; Grill-Spector and Malach 2001; Kourtzi and Huberle 2005; Kourtzi and Kanwisher 2001; Kourtzi et al. 2003; Murray and Wojciulik 2004). In a typical fMRI adaptation experiment, a pair of stimuli is presented in succession, with the second stimulus serving to probe the effects of adaptation caused by the first. The second may differ from the first in some stimulus dimension, such as spatial position, orientation, or size. If the fMRI response to the pair of stimuli is greater when the stimuli differ, it is inferred that the change along the varied stimulus dimension has recruited a separate, less-adapted neuronal subpopulation. It follows that the voxels showing this release from adaptation contain subpopulations of neurons selective to that stimulus dimension.

FMRI adaptation has been used to study selectivity of higher visual areas with robust results. For example, Grill-Spector and Malach (2001) showed that the presentation of a successive pair of identical faces but differing in either size or position produced similar adaptation effects in the lateral occipital cortex as presenting the same face twice. However, varying the viewpoint of the face produced a larger response. This is interpreted as

evidence of neurons in the lateral occipital cortex that are insensitive to size and position of a face, but are sensitive to viewpoint.

Such an interpretation of fMRI adaptation results depends on a variety of assumptions about the selectivity of the underlying neurons, their susceptibility to adaptation, and the neurophysiological basis of the fMRI signal (see Krekelberg et al. (2005)). Although fMRI-adaptation is most often used in higher visual areas, this technique needs to be validated in earlier visual areas that contain populations of neurons with response properties that are much better understood.

Interestingly, fMRI adaptation in early visual areas do not always show the expected results. Boynton and Finney (2003) found orientation-specific adaptation in extrastriate areas, but found no difference in fMRI adaptation effects in V1 despite the vast electrophysiological evidence that V1 neurons are orientation and pattern sensitive (Hubel and Wiesel 1962; Movshon and Lennie 1979; Muller et al. 1999). While this study presented brief 1 second stimuli, other studies have utilized a longer adaptation duration to reveal adaptation responses in V1 proportional to the angular difference between the adapter and test stimulus (Fang et al. 2005). Thus it appears that orientation-selective fMRI adaptation in V1is dependent on stimulus duration.

A recent study found spatially-specific but not orientation-specific adaptation effects in V1 (Murray et al. 2006) suggesting that some adaptation effects may be solely vascular in origin. It is possible that fMRI adaptation

may work because of nonlinear neurovascular coupling instead of neuronal adaptation. That is, the fMRI response might show a release from adaptation because the new stimulus excites a subpopulation of neurons that has a different, fresh vascular supply. Such a mechanism would show stimulus-specific fMRI-adaptation without neuronal adaptation (Krekelberg et al. 2006a).

One way to validate the fMRI adaptation technique is to compare fMRI adaptation results to the effects of adaptation on psychophysical measurements (Boynton and Finney 2003). A stimulus-specific adaptation effect measured psychophysically implies that there is neuronal selectivity to the stimulus dimension of interest somewhere in the brain. Comparing psychophysical and fMRI adaptation results can not only support the hypothesis that fMRI adaptation is neuronal in origin, but also shed light on the neuronal representation of the stimulus associated with the psychophysical task.

In this study, we utilized changing the direction of motion of the stimulus to tease out neuronal and hemodynamic contributions to the adapted fMRI signal in relatively well-understood visual areas. We used a rapid, event-related design to measure the response to pairs of sinusoidal grating stimuli moving in the same, orthogonal, and opposite direction. We find that in V1 and extrastriate areas, the fMRI response to the second stimulus is smaller than the first. In all visual areas, we observed a larger fMRI response in the

orthogonal and opposite conditions relative to the same condition. In all areas except MT+, the fMRI response to the different conditions was closely mirrored by psychophysically derived speed discrimination thresholds for a test stimulus following an adapter grating. Our results suggest that motion-specific fMRI adaptation in visual areas has both neuronal and vascular components.

## 3.3 Material and Methods

### 3.3.1 Subjects

Eight paid subjects participated in the fMRI study and nine paid subjects participated in the psychophysical study. Seven of these subjects (one was an author, A.S.T.) participated in both the fMRI and psychophysical studies. All subjects indicated informed written consent in accordance with the Salk Institute Human Subjects Review Board guidelines.

### 3.3.2 fMRI stimulus presentation apparatus

Stimuli for the fMRI experiments were generated on an Apple PowerMac G4 laptop computer (Apple Computers, Cupertino, CA) using Matlab version 5.2 (MathWorks, Natick, MA) and the Psychophysics Toolbox version 2.31 (Brainard 1997; Pelli 1997). Images were then projected onto a back-projection screen using an NEC Solutions (Itasca, IL) LT157 liquid crystal display projector fitted with a zoom lens (806MCZ123; focal length, 187–312 mm; Buhl Optical, Rochester, NY). Viewing distance was 22 cm. Projector refresh rate was 60 Hz, and the mean luminance was 50 cd/m2. Projector

gray scale values were gamma-corrected with respect to luminance using a photometer. Subjects lay supine in the bore of the MRI scanner and viewed the image on a screen near the subject's chest through a mirror mounted to the receive coil above the subject's eyes. A bite bar stabilized the subject's head.

### 3.3.3 fMRI stimuli

All stimuli used in the fMRI experiments were gratings of 100% contrast moving at 15 deg/s. The moving gratings were restricted within an annulus consisting of an outer radius of 6° and an inner radius of 1° (figure 3.1A). Gratings were oriented either vertically or horizontally, with a spatial frequency of 1 cycles/°, and lasting 333 msec (20 frames). A fixation point was placed in the center of the visual field, and uniform gray field with the same mean luminance of the grating surrounded the stimulus. Trials in the fMRI experiment consisted of either a single grating stimulus or pairs of grating stimuli separated by 100 msec. The second stimulus of each pair was oriented to the same, orthogonal, or opposite direction of motion to its first stimulus (figure 3.1B). A uniform gray field of same mean luminance as the gratings with a central fixation point (radius 0.1°) was presented between stimulus presentations. Each trial lasted 3 sec. An fMRI stimulus scan consisted of a 15 sec blank period, followed by 124 trials, lasting a total of 3 x 124 + 15 = 387 sec. Each experimental session consisted of a reference scan (see below), followed by 8 experimental scans. The motion of direction for the

first stimulus was held constant within an experimental scan. Five stimulus types were shown within each scan, made up same, orthogonal and opposite direction pairs, the adapter alone, and a blank.

The order of the five stimulus types was determined by using an m-sequence (Buracas and Boynton 2002) with an order of 5 and power value of 3. M-sequences are perfectly counterbalanced pseudorandom sequences where trials from each stimulus type are preceded equally as often by trials from each of the other stimulus types. The motion of direction for the first stimulus was counterbalanced across the 8 experimental scans in an fMRI scan session. Subjects passively fixated throughout the scan.

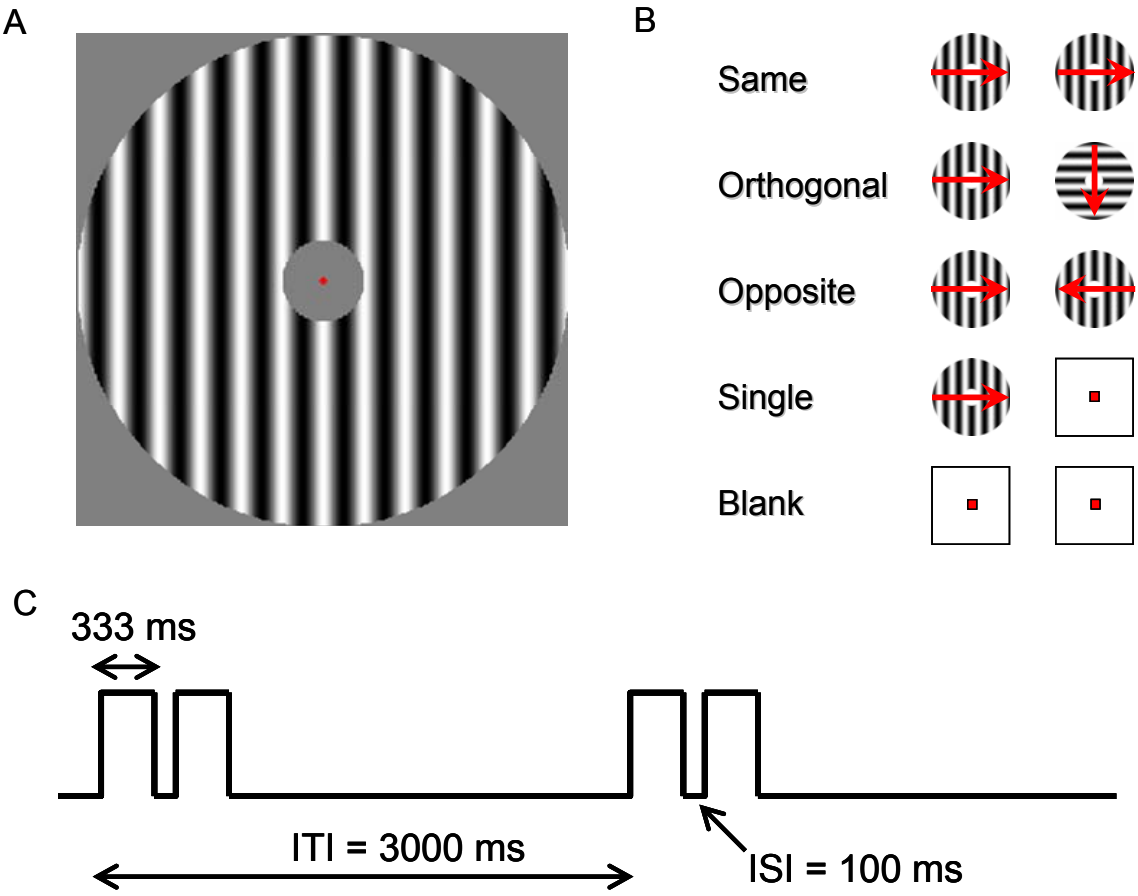


Figure 3.1: Stimulus diagram for fMRI experiments. Subjects viewed 333 msec duration moving gratings restricted within an annulus (A) presented in successive pairs, alone, or a blank (B). An intertrial interval (ISI) of 100 msec was used when successive pairs were presented. A new trial began every 3 sec (C). Pairs had the same, orthogonal, or opposite direction of motion.

### 3.3.4 fMRI data acquisition

fMRI data were acquired using a GE (Waukesha, Wisconsin) Signa Excite 3 Tesla whole body system scanner with a body transmit coil and an eight channel receive coil. During each experimental scan, 248 temporal frames were acquired over 372 sec (repetition time, 2 sec; flip angle, 90°; 24 interleaved slices of 4 mm thickness and 4 x4 mm resolution; field of view, 250 mm) using a low-bandwidth echo-planar imaging sequence (62.5 kHz). FMRI data from the first 15 sec was discarded to avoid the effects of magnetic saturation and visual adaptation. Four scan sessions with eight experimental scans per session were acquired from each subject. Each session also included one reference scan with 224 temporal frames acquired over 336 sec (repetition time, 2 sec; flip angle, 90°; 24 interleaved slices of 4 mm thickness and 4 x 4 mm resolution; field of view, 250 mm) using a low-bandwidth echo-planar imaging sequence (62.5 kHz). Retinotopic reference scans designed to identify V1, V2, V3, V3A, V4V, and an MT+ reference scan were obtained in a separate session. Each scanning session ended with an anatomical scan (magnetization-prepared rapid gradient echo, 1 x 1 x 1 mm resolution) using a standard T1-weighted gradient echo pulse sequence. Anatomical scans were used to align functional data across multiple scanning sessions to a subject's reference volume.

### 3.3.5 fMRI region of interest selection

Occipital visual areas V1, V2, V3, V3A, V4V, and MT+ were defined using standard retinotopic mapping and cortical-flattening techniques as described previously (Boynton et al. 1999; Engel et al. 1994; Sereno et al. 1994). Regions of interest within these predefined visual areas were selected by means of a reference scan that was run at the beginning of each session. Subregions within the predefined visual were selected based on the response to a high-contrast flickering checkerboard pattern subtending the same region of the visual field as the stimuli used in the main experiments (counterphase-modulated checkerboard flickered at 8 Hz). The flickering checkerboard was presented in alternation with a uniform gray field for eight blocks of 21 sec cycles (after discarding the initial 21 sec of data). For subsequent analysis, we chose voxels that correlated ($r > 0.20$) with an eight cycle sinusoid (using a fast Fourier transform) and had a temporal phase lag with respect to stimulus no larger than ~ 10 seconds. This procedure resulted in selecting well-localized foci of activation within the original contiguous set of voxels covering each visual area. Area MT+ was identified using standard techniques (Engel et al. 1994; Sereno et al. 1995) by measuring fMRI responses to high-contrast dot patterns (white dots on a black background) that alternated between moving (radially inward and outward) and stationary. Area MT+ was selected as a contiguous group of voxels lateral to the parietal–occipital sulcus and

beyond V1–V3, with a time series that correlated ($r$ > 0.2 within a 10 sec lag time) with the temporal alternation (moving vs stationary) of the stimulus.

### 3.3.6 fMRI data analysis

fMRI data from voxels which responded to the reference scan ($r$ > 0.2 ) were analyzed. The maximum likelihood estimates of the hemodynamic response (HDR) to the four stimulus types were calculated within subject, visual area, and fMRI scan, correcting for up to a fourth-order drift in noise. HDR estimates were averaged together for each stimulus condition across scans and sessions. The signals from left and right halves of the same visual area were averaged together within a subject. Since the stimuli presented were brief and we expect only a difference in amplitude between conditions and do not expect a significant change in response shape, the HDR estimates across same, orthogonal, and opposite conditions were averaged in a given region of interest for each subject. Smooth curves were fit to the fMRI responses in a given region of interest using a parametric function, which is the difference of two gamma functions:

$$h(t) = h_1(t) - h_2(t) + k,$$

where:

$$h_i(t) = \frac{((t - \delta_i)/\tau_i)^{(n_i - 1)} e^{-(\tau_i - \delta_i)/\tau_i}}{\tau_i (n_i - 1)!}$$

The parameters $n_1$ *and* $n_2$ were set to 4 and 8, respectively, and the remaining five parameters were allowed to vary freely for each curve. Note that each

component of this function, $h_1$ and $h_2$, has the same parametric form as used in previous fMRI studies (Boynton et al. 1996). The difference between two gamma functions predicts a biphasic response when the second function, $h_2(t)$, has a slower time course than the first. This smooth parametric function provides a continuous description of the curves and provides an estimate of parameters such as maximum height. Within a given visual area for each subject, the amplitudes to the different stimulus conditions were determined by the best-fitting parametric function described above.

### 3.3.7 Psychophysical stimulus presentation apparatus

Psychophysical speed discrimination experiments were performed outside the scanner in the laboratory under conditions designed to match the fMRI stimulus conditions. Subjects viewed stimuli using the same computer, projector model, back-projection screen material, and viewing distance as used during fMRI data acquisition. Subjects viewed stimuli on a back-projection screen using a chin rest while sitting in an upright position in a dark room. As in the fMRI studies, the video refresh rate was 60 Hz, and the mean luminance of the stimulus was 50 cd/m2. Subjects were given a response box synced to the computer to record behavioral responses.

### 3.3.8 Psychophysical stimuli

The adapting stimulus in the psychophysical experiments was identical to that of the fMRI experiments (grating moving at 15 °/s restricted with an annulus with an outer radius of 6° and inner radius of 1°; 1 cycles/°, 333 msec

duration). Unlike the fMRI experiments, test stimuli were gratings moving within disks (2° radius, 1 cycle/°, 100% contrast). The test stimuli were located left and right of fixation and centered within the same spatial location subtended by the adapting annulus (figure 3.2). The test stimuli moved at different speeds but average speed of the test stimuli was equal to the adapting stimulus. The two test stimuli moved in the same direction and lasted 333 msec. A white fixation point (0.1° radius) was placed in the center of the visual field, and uniform gray field with the same mean luminance of the test gratings surrounded the stimulus. Trials in the psychophysical experiment consisted of either the test stimuli alone or pairs of an adapter stimulus followed 100 msec by the test stimuli. The adapter stimulus of each pair was oriented to the same, orthogonal, or opposite direction of motion to the test stimuli. A uniform gray field of same mean luminance as the gratings with a central fixation point was presented between stimulus presentations. Each trial lasted 3 sec. An 80 msec auditory beep at 850 Hz was presented 433 msec before the test stimuli to cue the subject to the beginning of the trial. The fixation point simultaneously flashed for 80 msec. A psychophysical run consisted of 40 trials crossed with 4 conditions, lasting a total of 3 x 40 x 4 = 480 sec. Each psychophysical session consisted of 8 psychophysical runs. The motion of direction of the test stimuli was held constant within a psychophysical run and was counterbalanced across the 8 psychophysical runs in a session. The order of conditions presented was determined by a

pseudorandom sequence. Subjects fixated throughout the task and received immediate feedback on trial performance.

### 3.3.9 Psychophysical methods

Speed discrimination thresholds were obtained using a three-down, one-up staircase procedure with a two-alternative spatial forced-choice trial structure. On each trial, the subject's task was to indicate the faster moving test stimulus (left or right of fixation) with a key press. Subjects had to respond within a 1000 msec response interval; otherwise, the trial was discarded. The fixation point briefly changed colors after each trial to inform the subject if the response was correct (green), incorrect (red), or not recorded in time (yellow). Within each test condition, the speed difference of the two test stimuli on the next trial of that particular test condition was reduced after three correct responses in a row and increased after a single incorrect response. Each staircase consisted of 40 trials. All four conditions were tested within one psychophysical run and the order of conditions presented was psuedorandomized using an m-sequence. Subjects were not informed that the direction of movement for the test stimuli was held constant throughout a single psychophysical run and that the direction of the adapter varied. In subsequent runs, the direction of the test stimulus rotated 90 degrees. A psychophysical session consisted of eight runs, and all subjects participated in at least 4 sessions.

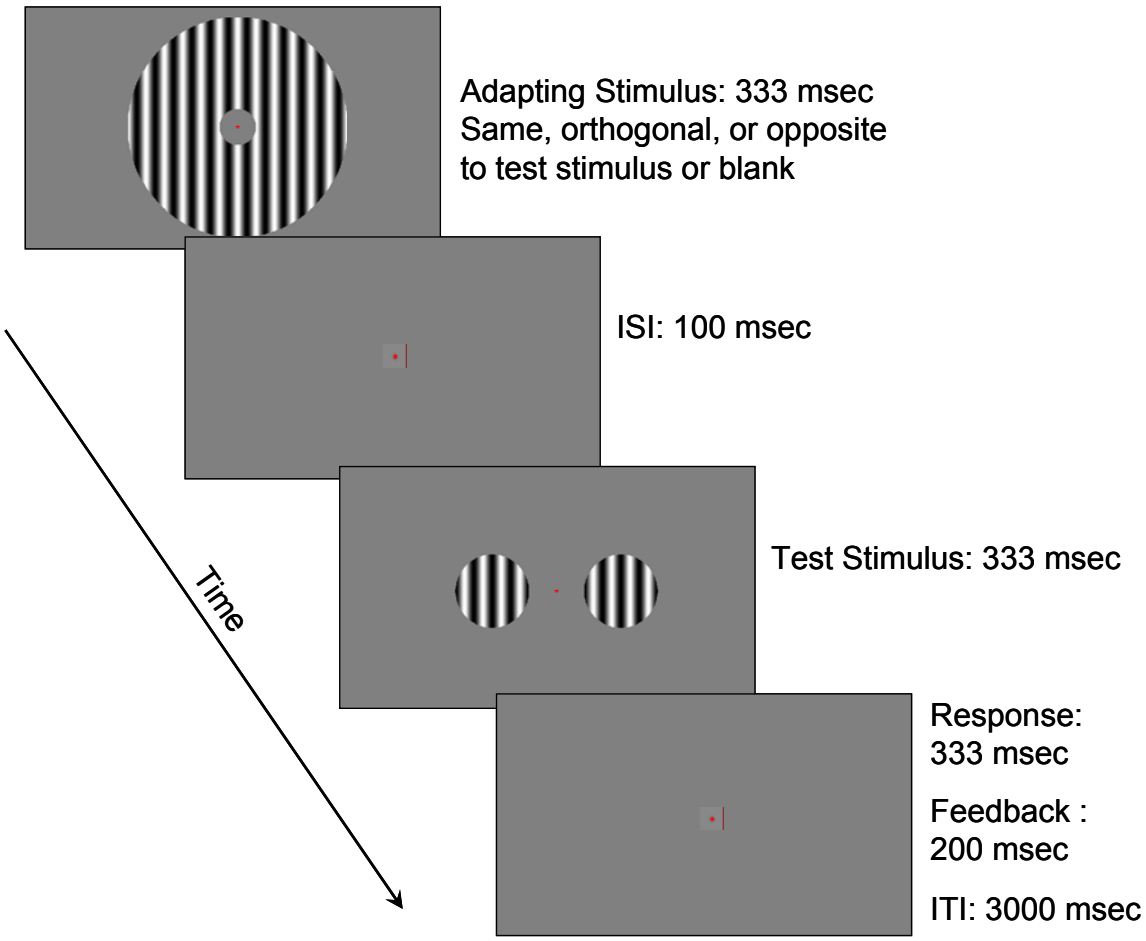


Figure 3.2: Stimulus diagram for the psychophysical experiments. Subjects viewed 333 msec duration test stimuli consisting of moving gratings within two disks. The gratings moved in the same direction but at different speeds and subjects performed a 2-AFC speed discrimination. Either a blank or a a 333 msec duration moving grating restricted within an annulus and enveloping the spatial locations of the test stimuli was presented before the test stimuli. An intertrial interval (ISI) of 100 msec was used when successive pairs were presented. A new trial began every 3 sec (C). The adapting stimulus moved at the average speed of the test stimuli and had the same, orthogonal, or opposite direction of motion. Subjects received immediate feedback following each trial.

Psychometric functions (percentage correct as a function of contrast) were fit with a Weibull function using a maximum likelihood estimate. The speed discrimination that predicted 79% correct performance was defined as the speed discrimination threshold. Baseline speed discrimination detection thresholds were obtained without an adapting stimulus. In the adapting conditions, the adapting stimuli were identical to those used in the fMRI experiments. Thresholds were calculated for the approximately 32 runs per condition per subject. Thresholds falling outside 1.5 standard deviations from the mean were excluded to provide a robust estimate of average threshold. Speed discrimination thresholds were inverted to obtain a sensitivity measurement and averaged within subjects. The sensitivity ratio for each condition was defined as the ratio of the sensitivity for that condition and the baseline speed discrimination sensitivity. Error bars for the sensitivity ratio represent standard error.

## 3.4 Results

### 3.4.1 fMRI adaptation experiment

Figure 3.3 shows hemodynamic responses for the four conditions in the event-related fMRI experiment averaged across all sessions and subjects. Results are shown in visual areas V1, V2, V3, V3A, V4V, and MT+. The cyan curve shows the response to the *single* stimulus condition, and the blue, green and red curves correspond to the *same*, *orthogonal*, and *opposite* condition, respectively. As expected, the *single* condition produces the smallest

response, while the other three conditions produce larger, but similar responses. Amongst the responses to the paired stimuli, the same condition produces the smallest response in each of the visual areas examined.

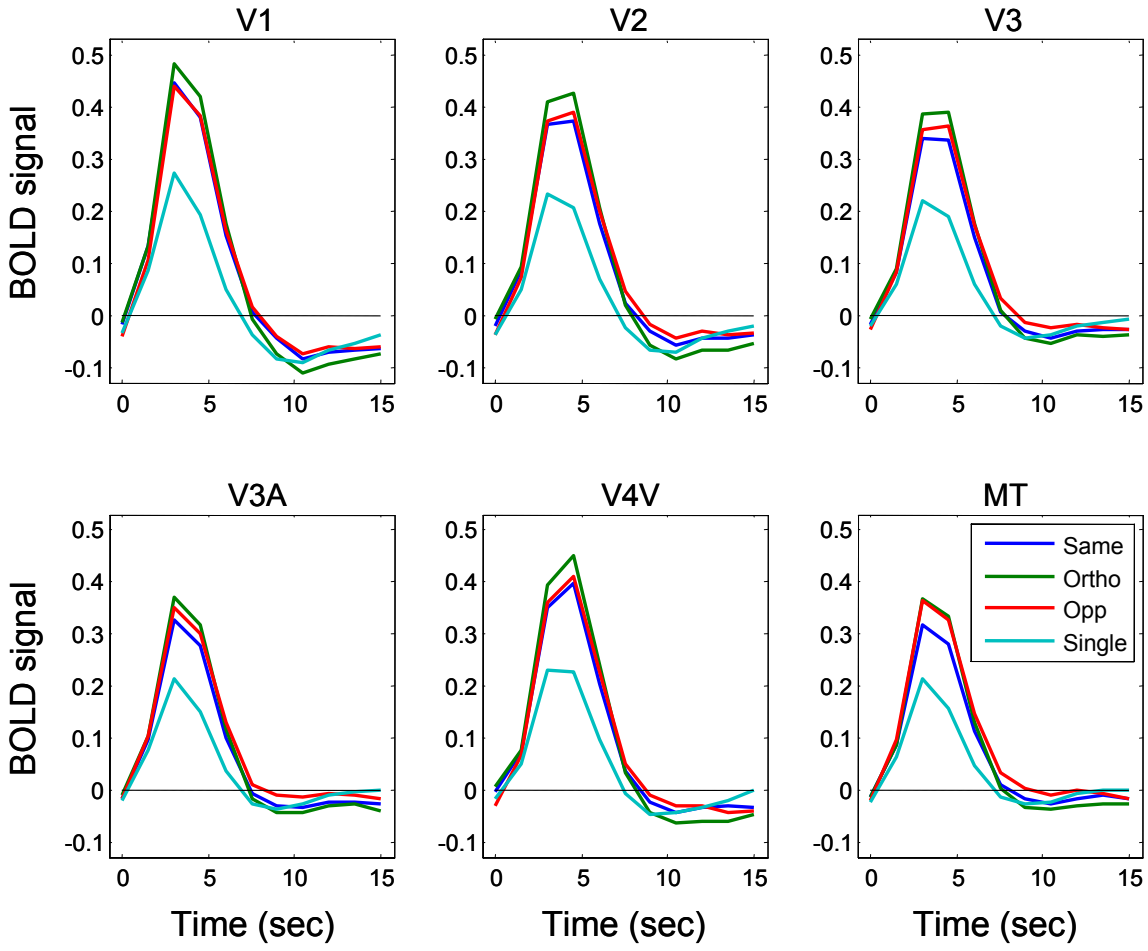


Figure 3.3: Hemodynamic responses to adaptation stimuli. Hemodynamic responses were measured in areas V1, V2, V3, V3A, V4V, and MT+ for the four stimulus conditions in the event-related fMRI experiment. Responses are averaged across all subjects and scan sessions. The cyan curve shows the response to the single stimulus condition, and the blue, green and red curves correspond to the same, orthogonal, and opposite condition, respectively.

To quantify the magnitude of these responses, we fit a template hemodynamic response function to each of the curves for each subject and within each visual area (see Methods). The amplitude, in percent signal change, was defined as the highest point on the fitted curve. Figure 3.4 shows bar graphs of these amplitudes for the four conditions in the six visual areas, averaged across all eight subjects. Error bars represent standard errors of the mean across subjects. In all areas, the *single* condition produces the lowest amplitude, as expected.

In a linear system, the *same* condition should produce roughly double the amplitude response as the *single* condition. The red-dashed lines in figure 3.4 represent twice the *single* condition's amplitude. As can be seen, in all visual areas, amplitudes from the *same* condition fall below this line. Note that this could be caused by either a nonlinearity in the hemodynamic coupling process, or an adapted neuronal response to the second stimulus. The amplitudes from the *orthogonal* and *opposite* conditions are larger than that from the *same* condition. Depending on the visual area, these amplitudes are nearly as large as the doubled amplitude from the *single* condition. This implies that there is a release from adaptation, possibly caused by the second stimulus stimulating a second, unadapted subpopulation of neurons. These results are consistent with a small amount of neuronal adaptation followed by a roughly linear hemodynamic coupling process.

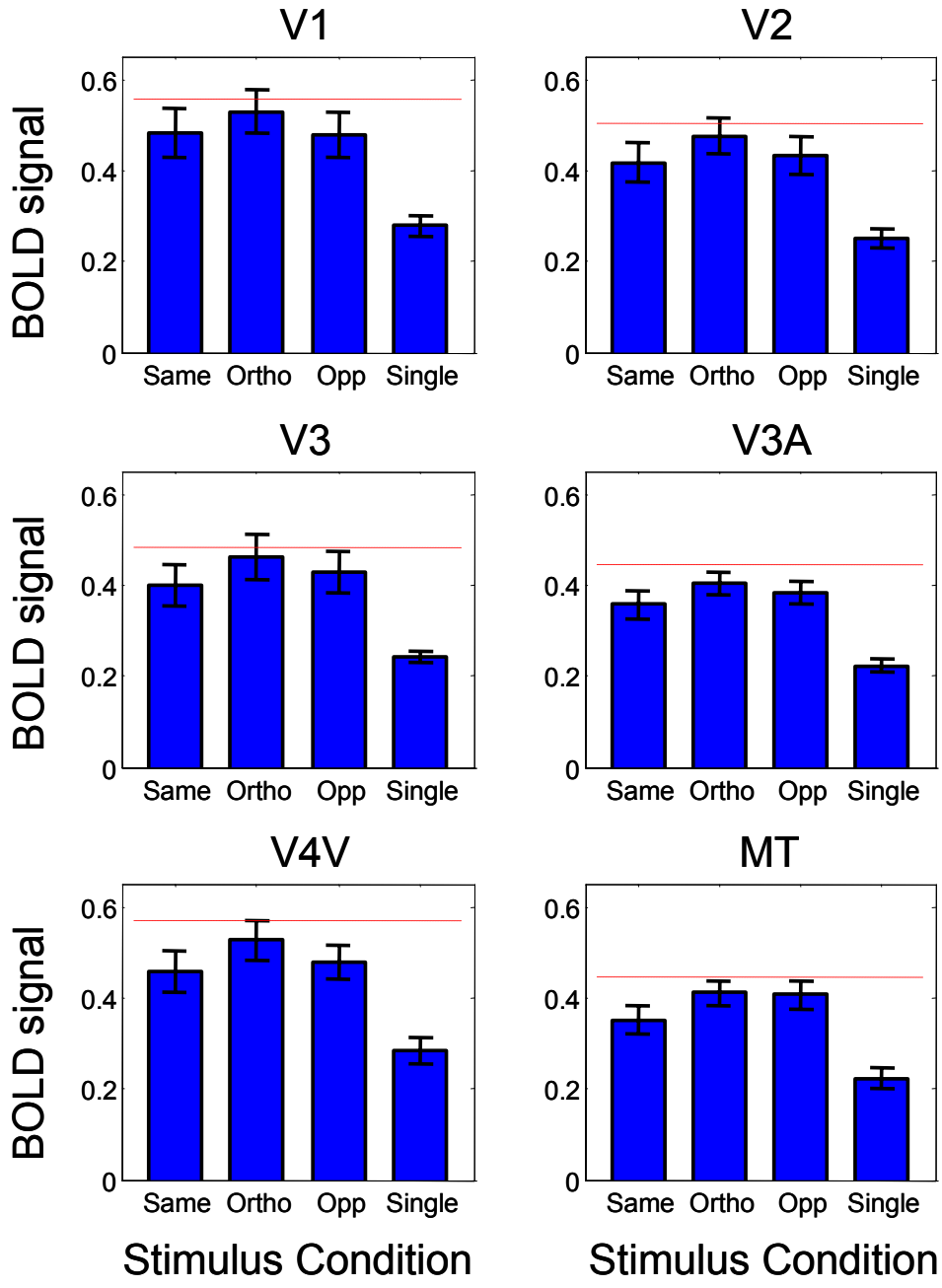


Figure 3.4: Peak amplitudes for the hemodynamic responses. Peak amplitudes were quantified from a template hemodynamic response function in areas V1, V2, V3, V3A, V4V, and MT+ for the four stimulus conditions. Amplitudes are in percent signal change and are averaged across all subjects. Error bars represent standard errors of the mean across subjects. In all areas, the *single* condition produces the lowest amplitude, as expected. The red-dashed lines represent twice the single condition's amplitude.

The amplitudes for the *same*, *orthogonal*, and *opposite* conditions are quite similar. However, a 3-way analysis of variance test for the three conditions (*same*, *orthogonal*, and *opposite*), six visual areas (V1, V2, V3, V3A, V4V, and MT+), and subjects as a random effects variable shows a significant main effect of condition ($p < 0.005$). Thus, there is a reliable difference in adaptation effects across the three conditions.

There was also a significant interaction between visual area and condition ($p < 0.001$). So although there are not large differences in the adaptation effects between say, V1 and MT+, these differences are reliable. All visual areas other than MT+ show the greatest release from adaptation for the *orthogonal* condition. This suggests that changing both the orientation and the direction of motion excites a more independent subset of neurons than just changing the direction of motion. This is consistent with these visual areas being selective to both orientation and direction of motion. Area MT+ shows similar adaptation effects in the *orthogonal* and *opposite* conditions. This could be because area MT+ contains predominantly direction-selective neurons with fairly narrow tuning, so that once the stimulus is rotated 90 degrees, a whole new subpopulation is excited, so rotating to the full 180 degrees results in no further release from adaptation in the population of neurons.

Because the error bars in figure 3.4 represent variability across subjects, they over-represent the variability associated with using subjects as

a random effects variable. To better represent the reliability of the differences in adaptation effects across the *same*, *orthogonal*, and *opposite* conditions, it makes sense to normalize each subject's amplitude by the response with respect to the *single* condition. This compensates for overall differences in the amplitudes of the fMRI response for each subject. Figure 3.5 shows the amplitudes from figure 3.4, after dividing by *twice* the *single* condition (red dashed lines in figure 3.4), averaged across all eight subjects. Now, a value of one indicates twice the response to the *single* condition, and therefore linearity. The pattern of adaptation effects is similar to that seen in figure 3.4, but the variability (as seen by the error bars) is slightly smaller. Figure 3.5 shows small, but reliable differences in the amplitudes across the three two-pulse conditions.

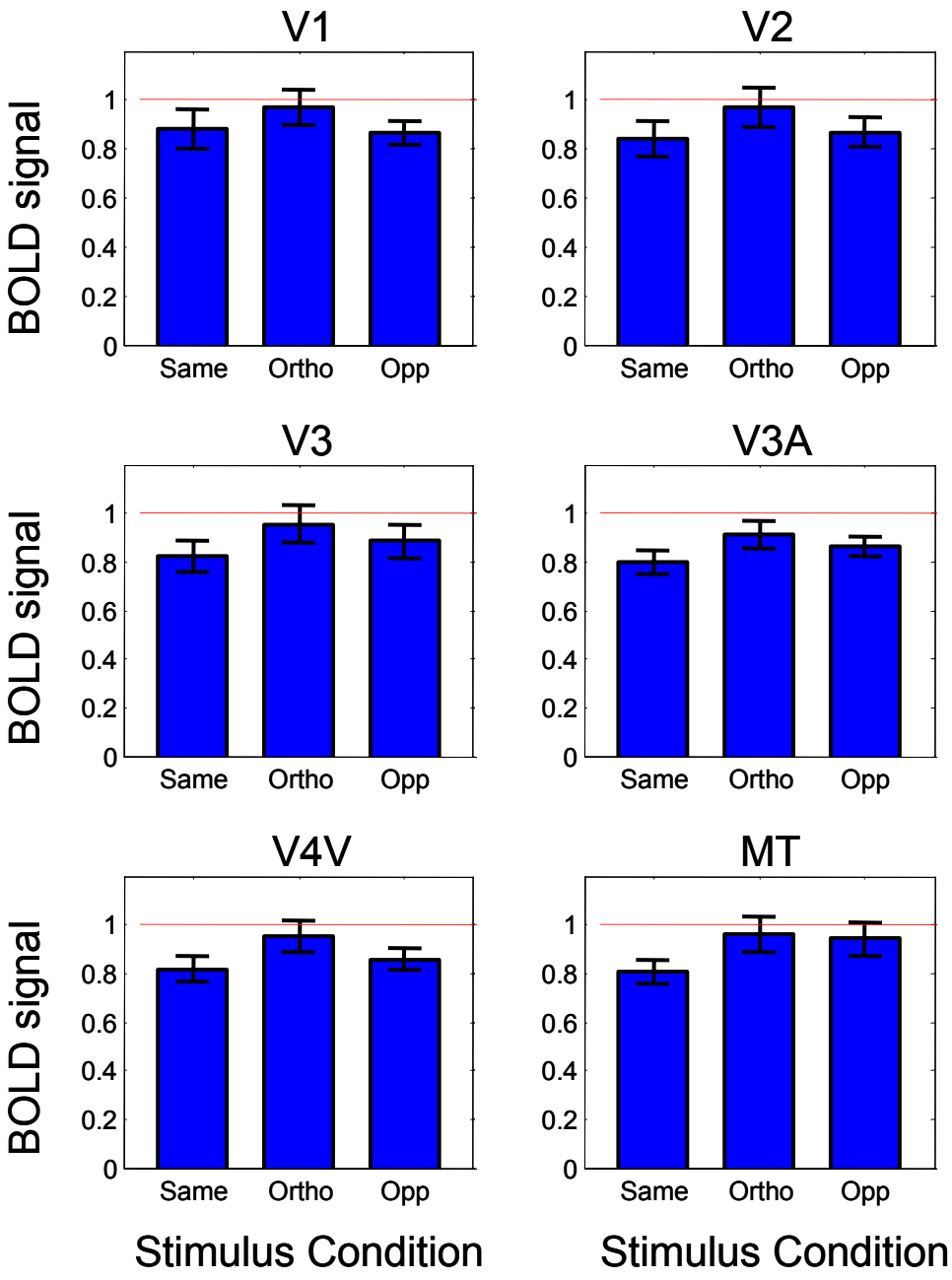


Figure 3.5: Amplitudes normalized to single condition. Amplitudes normalized by twice the single condition within each subject in areas V1, V2, V3, V3A, V4V, and MT+ for the three paired stimulus conditions. Normalized amplitudes are averaged across all subjects. Error bars represent standard errors of the mean across subjects. The red-dashed lines have a value of one and represent the response to twice the single condition.

### 3.4.2 Psychophysical experiment

Figure 3.6A shows speed discrimination thresholds, averaged across 9 subjects for the four conditions. The *single* condition is the threshold measured alone, without a preceding adapting stimulus, and serves as the baseline speed discrimination threshold. The other three conditions are the measured speed discrimination thresholds of the test stimulus following the presentation of an adapting grating moving in the *same, orthogonal*, or *opposite* direction of motion. Error bars represent standard errors of the mean across subjects. Figure 3.6B shows the reciprocal of the same threshold measurements, typically defined as *sensitivity*. Larger sensitivity values reflect lower psychophysical thresholds. Subjects are least sensitive in the *single* condition, followed by the *same*, *opposite*, and then the *orthogonal* conditions. Although these differences are small, a 2-way analysis of variance test for the three conditions (*same*, *orthogonal*, and *opposite*), and with subjects as a random effects variable shows a significant main effect of condition ($p < 0.0083$).

Figure 3.6C shows the psychophysical sensitivity measurements normalized by the *single* condition, which serves to account for the variability in overall threshold values within each subject. The pattern across the three adapted conditions remains the same, but the variability (as indicated by the error bars) is reduced. This shows that the direction of motion of the adapting

stimulus had a significant and reliable influence on the subsequent speed discrimination thresholds.

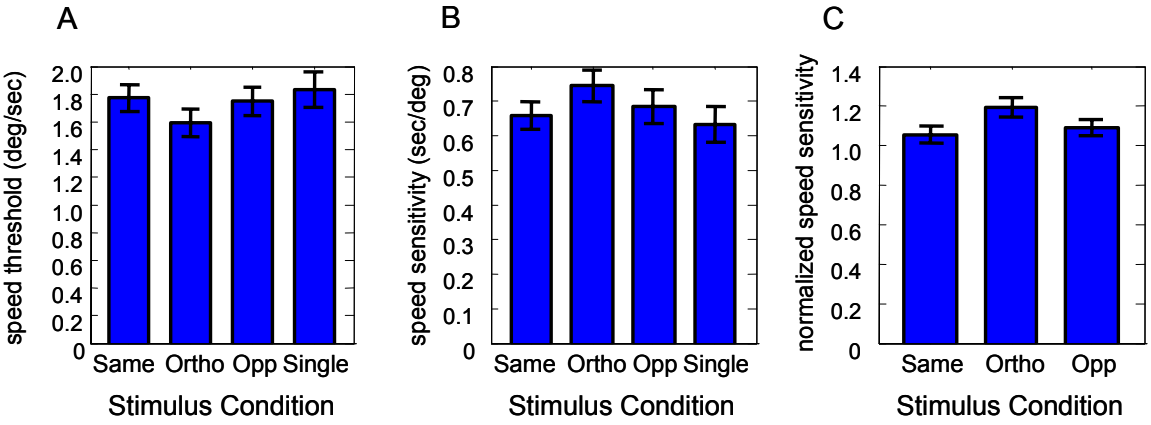


Figure 3.6: Speed discrimination thresholds and sensitivity. Speed discrimination thresholds at 79% correct performance are shown for the four stimulus conditions (A). The single condition is the threshold measured without a preceding adapting stimulus and serves as a baseline measurement of performance. The other three conditions represent performance with the presence of an adapter grating in the appropriate direction of motion. Thresholds were averaged across subjects, and error bars represent standard errors of the mean across subjects. Sensitivity measurements were obtained by taking the reciprocal of the thresholds (B). Within each subject, sensitivity measurements were normalized by the single condition (C). Sensitivity measurements were averaged across subjects, and the error bars represent standard errors of the mean across subject.

### 3.4.3 Comparing fMRI and psychophysical results

Our hypothesis linking our fMRI and behavioral measurements is that speed discrimination thresholds measured after the adapting stimulus reflects the adaptive state of the neurons representing the test stimulus. A greater amount of adaptation should lead to larger speed discrimination thresholds or

conversely, lower sensitivity. This is consistent with a simple ideal-observer model for speed discrimination, in which the observer monitors the response of a population of direction and speed-selective neurons in which the variance of the neuronal response is proportional to the mean. Larger neuronal responses lead to a more reliable representation of speed (because the mean response increases relative to the standard deviation). This model was supported in a previous study comparing fMRI responses to speed discrimination thresholds as a function of stimulus contrast (Buracas et al. 2005). In fact, the model predicts that speed discrimination thresholds should be inversely proportional to the population response. Therefore, sensitivity values should correlate directly with the strength of the fMRI adaptation results.

A comparison of the fMRI results in figure 3.5 to the psychophysical results in figure 3.6C shows that the amplitudes in the adapting conditions in the fMRI results fall below unity, while the sensitivity in the adapting conditions from the psychophysical results are greater than one. That is, thresholds in the *single* condition are *higher* than the thresholds measured after an adapting stimulus. This means that the speed discrimination thresholds in the unadapted, *single*, condition are poorer than predicted by the fMRI results.

We now focus on comparing fMRI results to the behavioral data for the three adapting conditions. Which visual areas best reflect the psychophysical data? Visual inspection shows a qualitative match between the normalized

behavioral sensitivity values in figure 3.6C and the normalized fMRI results in figure 3.5 in all areas except area MT+. One way to quantify this comparison is to calculate the correlation between the three adapting conditions between the two data sets for each visual area. Of course, a correlation value with three measurements will typically be high, but we can compare the measured correlation values with correlation values expected by chance.

Figure 3.7 shows the squared-correlation values (percent of variance accounted for) between the three fMRI adapting conditions in each visual area to the three sensitivity measures in the adapting conditions in the psychophysical experiments. All areas show high correlations except area MT+, in which only about 60% of the variance in the fMRI results are accounted for by the psychophysical data. To quantify these correlations statistically, a bootstrapping calculation was performed in which all of the fMRI measurements were pooled and sampled with replacement to generate simulated fMRI data sets. These sets were repeatedly correlated with the behavioral measurements. The numbers on the bars in figure 3.7 indicate the probability that a simulated, random data set correlated better with the psychophysical data than the observed data. Areas V2 and V4V show p-values of 0.0032 and 0.0011, respectively, indicating that it is highly unlikely that the fMRI results in these two areas correlate with the behavioral measurements this well by chance. Correlation analysis within subjects was also performed, however, within-subject correlation values for fMRI and

psychophysical data were not significantly different than between-subject correlation values.

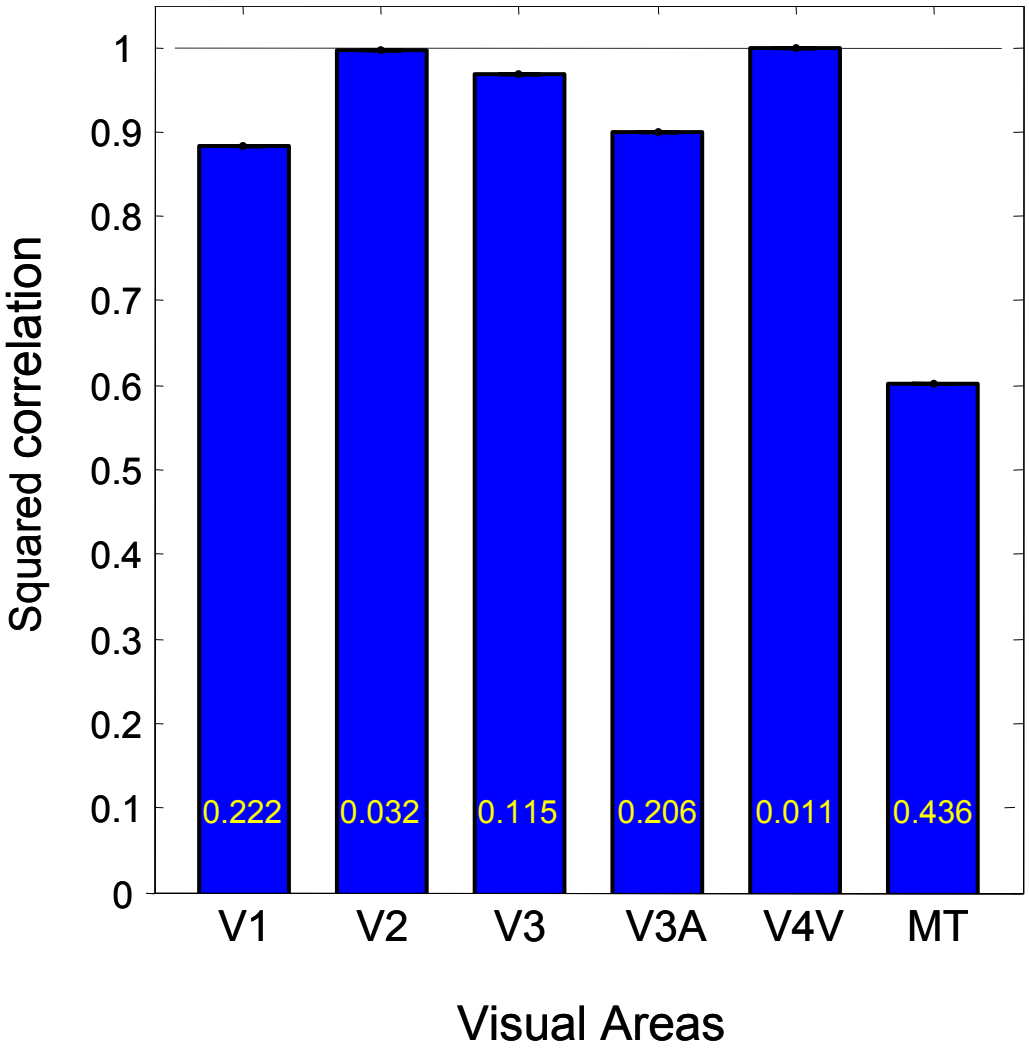


Figure 3.7: fMRI and psychophysical correlations. The bars represent correlations between the three fMRI adapting conditions (same, orthogonal, and opposite) in visual areas V1, V2, V3, V3A, V4V, and MT+ with the analogous conditions in psychophysics. Bootstrapping calculations were performed on all fMRI data, and the numbers on the bars represent the probability that a random data set correlated better than the observed data.

## 3.5 Discussion

### 3.5.1 Refractory Effects

Early fMRI studies found that the repetition of a single stimulus produces smaller and smaller responses in the visual cortex (Dale and Buckner 1997). These early results were typically interpreted as evidence of a nonlinearity, or refractory effect, in the hemodynamic coupling process. These refractory effects are quite large when the hemodynamic response is allowed to recover between trials (after 15-20 seconds). For example, Boynton and Finney (2003) found that the effective response to the second stimulus to be around half that of the first, which is typical of other studies with similar timing parameters (Dale and Buckner 1997; Huettel and McCarthy 2000; Huettel et al. 2004). An alternate explanation for these refractory effects is that the underlying neuronal response is adapting in response to the first stimulus, while the fMRI signal follows a faithful linear convolution of the underlying neuronal response (Boynton et al. 1996). However, a 50% reduction in the neuronal response to a brief stimulus seems large, which suggests that a large component of the refractory effect is hemodynamic in origin.

In contrast, the present study found relatively small refractory effects when the same stimulus was presented twice. The effective fMRI response to the second stimulus was about 80% of the response to the first stimulus presented alone (see figure 3.5). An important difference between the studies showing large refractory effects and ours is that we used a rapid event-related

design in which each trial began every few seconds, which may be measuring the BOLD signal under more steady-state hemodynamic conditions. Rapid event-related adaptation designs may reflect more influence from neuronal adaptation, rather than hemodynamic refractory effects.

### 3.5.2 Orientation-specific adaptation in V1

If fMRI adaptation measures stimulus-specific selectivity, then the one stimulus and brain area that should show a positive result should be orientation in V1. However, evidence of orientation-specific adaptation of the fMRI response in V1 is mixed. The expected orientation-specific adaptation effects are found in V1 with long duration adapting stimuli (Fang et al. 2005; Larsson et al. 2006; Tootell et al. 1998). However, using a rapid adaptation paradigm (pairs of 1-second oriented gratings) Boynton and Finney (2003) found no orientation-specific adaptation in V1. Similarly, Fang et al. (2005) also failed to find orientation-specific fMRI adaptation in V1 with brief stimuli. Both of these studies allowed the hemodynamic response to recover between trials. In contrast, using a rapid event-related design, (Kourtzi and Huberle 2005; Kourtzi et al. 2003; Krekelberg et al. 2005) did find a small orientation-specific fMRI adaptation in V1 with stimulus presentations as short as 300 msec. Perhaps, as stated above, rapid event-related designs emphasize neuronal adaptation over hemodynamic refractory effects.

Unlike for orientation however, fMRI adaptation results using moving stimuli do seem to show clear direction-selective adaptation with brief stimuli.

Huettel et al. (2004) found a near complete recovery of the fMRI response in both the pericalcarine and in MT+ with pairs of stimuli moving in opposite directions. Like Huettel et al. (2004), we found that reversing the direction of motion led to a recovery of the fMRI response in area MT+. However we did not find much recovery in V1, V2, V3, V3A or V4V.

In the present study, we also included an orthogonal condition, in which the second stimulus was rotated by 90 degrees compared to the first. In contrast to the opposite condition, the orthogonal condition led to nearly complete recovery from adaptation in all of the reported visual areas. Thus, area MT+, which presumably contains a large proportion of direction-selective neurons, had complete recovery with both a 90 and 180 degree rotation in the direction of the second stimulus. In other visual areas, however, a 90-degree rotation leads to recovery, but 180 degrees does not. This is consistent with these areas containing a large proportion of orientation, but not direction-selective neurons.

### 3.5.3 Comparison with psychophysics

We used a speed discrimination task to test the state of adaptation after the presentation of the first stimulus. We also measured speed discrimination thresholds without an adapting stimulus. Based on the fMRI results, we expected speed discrimination thresholds without an adaptor (the *single* condition) to be lower than those with an adaptor. However, the presence of an adapting stimulus actually *lowered* thresholds.

There are a variety of possible explanations for this. One is that in the psychophysical *single* condition, subjects may be less certain about when the stimulus is appearing. Despite the auditory cue for the onset of the trial, the adaptors in the adapting conditions could have served as a prime to reduce the temporal uncertainty of the following target stimulus, leading to overall better discrimination thresholds. A second explanation is that the psychophysical sensitivity values in figure 3.6B might accurately reflect the relative neuronal responses, and the reduction in the fMRI responses in the adapting conditions reflects an overall refractory effect in the BOLD signal. It is perhaps surprising that the neuronal response to the second stimulus should exceed the first, but recall that the second stimulus is attended, while the adapting stimulus is ignored. fMRI results in the human visual cortex show that attention can increase the response to a stimulus in early visual areas by about 10% (Gandhi et al. 1999). This is not far from the increase in sensitivity values in the adapting conditions, compared to the *same* condition (see figure 3.6B). Such attentional effects should not be seen in the fMRI results since these experiments were conducted under passive viewing conditions.

Leaving this psychophysical and fMRI *single* conditions aside, the pattern of psychophysical results across adapting conditions matches very closely with the pattern of fMRI adaptation results in areas V2 and V4V, and matches poorly with fMRI results in area MT+. Given that this is a speed discrimination task, it is perhaps surprising that our best matches between

psychophysics and fMRI were found outside of MT+. There are two previous studies that compared fMRI adaptation effects with psychophysical thresholds. Boynton and Finney (2003) found orientation-specific psychophysical effects for contrast detection, which like the present study, match most closely with fMRI responses in V4. Using short-duration adaptors, Fang et al. (2005) also found orientation-specific effects on contrast detection thresholds, which were most consistent with fMRI results in V3A and V4. Note that these results are in contrast with a recent study showing that like fMRI responses in MT+, the pattern of speed discrimination thresholds is unaffected by stimulus contrast (Buracas et al. 2005).

### 3.5.4 Comparison with electrophysiological evidence of motion adaptation

A number of electrophysiological studies of motion adaptation in area MT in macaques have focused on the reduction in firing rate after adaptation in the preferred direction (Kohn and Movshon 2003; Petersen et al. 1985; Van Wezel and Britten 2002). Motion adaptation in macaque MT also narrows speed tuning curves and enhances speed discrimination (Krekelberg et al. 2006b). While adaptation in the preferred direction has been widely accepted to reduce the firing rate in MT, the effect of adaptation in the null or antipreferred direction is not as clear. One group found adaptation responses that were inconsistent or did not change the response (Van Wezel and Britten 2002), another group found enhancement of responses to the preferred

direction after long-term (20 second) null adaptation (Petersen et al. 1985), while a third group found that adapting the null direction reduced the suppression of the preferred response but did not increase the overall response (Kohn and Movshon 2003). This third group presented 1 second duration drifting gratings after a 5 second top-up adaptation stimuli and demonstrated that much of the reduction in firing rate after adapting in the preferred direction can be attributed to a change in the contrast gain, and that this effect was spatially specific within the MT cell's receptive field, suggesting that these effects occur earlier in visual processing and not in MT. Contrast gain changes are then most likely inherited from V1 or synaptic depression of feedforward inputs to MT. Interestingly, they also demonstrated that adapting the cell in the null direction has little effect on the firing or response to the preferred direction; however, adapting the null direction weakens the strength of the opponent input to MT neurons. This reduction in suppression is reflected by an effective shift in contrast sensitivity. If null adaptation does not increase the firing rate in the preferred direction, we would expect that the reduction in response in the preferred direction coupled with the lack of increased response in the null direction would reduce the overall level of activity in MT. These results are in contrast to a study which showed enhanced fMRI signal in hMT+ when experiencing the motion after effect (Huk et al. 2001).

Our fMRI results in MT+ which show a recovery from adaptation when the second moving stimulus is rotated 90 or 180 degrees relative to the adapting stimulus is consistent with Kohn and Movshon's findings. When the first and second stimuli move in the same direction, we see a reduction in fMRI signal as compared to a linear system. Presumably, with a longer duration of adaptation, we would see a larger degree of signal suppression. This observation is consistent with electrophysiological evidence of adaptation in the preferred direction of an MT cell and no change in signal with adaptation in the null direction. We must remember that fMRI is a population response and that these large stimuli will move in the preferred direction for some cells and in the null direction for others. When the second stimulus is rotated 90 degrees, we observe a release in adaptation in our fMRI results in MT+ because the average tuning bandwidth of MT cell is approximately 90 degrees (Albright 1984), and the second stimulus is exciting a fresh unadapted subpopulation of direction-selective neurons. When the second stimulus is rotated further to 180 degrees, we also observe a release in adaptation. This result is consistent with the first adapter acting as a null adapter in some of the MT+ cells. When the second stimulus is presented moving in the opposite direction (the preferred direction in this case), the opponent input is suppressed, and we observe a larger signal or a release from adaptation.

It has been demonstrated that adapting MT cells at their preferred direction reduces the direction-tuning bandwidth and adapting the cells to

near-preferred directions shifts the tuning curve toward the adapting direction (Kohn and Movshon 2004). Both null and orthogonal adapters evoked only a tiny response and adaptation did not have an effect on direction tuning (Kohn and Movshon 2004). The finding in MT where the adapted direction produces the least amount of reduction of the response is in contrast to adaptation studies in V1 which show the largest reduction in firing with respect to the adapting stimulus' spatial frequency, temporal frequency, or orientation (Muller et al. 1999). This means we see the largest reduction in response in V1 when the adapting and test stimuli are identical or similar but we see minimal reduction in MT. One group also investigated non-direction-selective cells in macaque V4 and elicited direction selectivity after a motion adaptation paradigm (Tolias et al. 2005) suggesting that area V4 receives direction-specific inputs from MT/V5 that are modulated by adaptation.

### 3.5.5 Stronger selective effects during constant stimulation

Using a rapid, event-related design seems to elicit the greatest amount of stimulus-selective fMRI adaptation (Fang et al. 2005; Huettel et al. 2004). Using this design, we were able to observe a release from adaptation in all visual areas. This is in contrast to earlier findings which did not observe orientation-selective adaptation in V1 but used a stimulus design which allowed the fMRI response to reach baseline with an intertrial interval of 24 seconds (Boynton and Finney 2003). While orientation-selective adaptation in V1 has been observed when using a long adaptation paradigm (Fang et al.

2005; Tootell et al. 1998), stimuli was constantly presented to the subjects, and the fMRI response was never allowed to return to baseline. Perhaps stimulus-selectivity is partly dependent on not only the presumed adaptation of neuronal subpopulations but on the state of the hemodynamic system. It appears that an activated hemodynamic state may be more optimal in observing selective fMRI adaptation than a well-rested one.

### 3.6 Conclusions

Using a rapid event-related fMRI adaptation paradigm, we found that all reported visual areas had a nearly complete recovery from adaptation when the second stimulus changed in direction from the first by 90 degrees. With a change of 180 degrees, this recovery remained complete only in area MT+, reflecting the direction selectivity of MT+ over the orientation selectivity of the other visual areas (V1, V2, V3, V3A and V4V). Psychophysical speed discrimination thresholds under adapting conditions similar to those used with fMRI found a pattern of results that most closely matched fMRI adaptation effects in V2 and V4V.

### 3.7 Acknowledgements

We thank Vivian Ciaramitaro for her assistance in event-related fMRI analysis.

The text of Chapter Three is a reprint of a manuscript being prepared for submission of which I am the primary author. It will be submitted as August S. Tuan and Geoffrey M. Boynton. “fMRI Adaptation to Motion in Human

Visual Areas is reflected in Behavioral Performance." *Journal of Neurophysiology*. 2006.

# Chapter 4

# Conclusions

## 4.1 Nonlinearity of the fMRI signal

We observed that the transient neuronal response may be modulated by increasing ramp duration, however, the fMRI nonlinearity to short stimulus durations still remains. The amount of overprediction in the fMRI response is approximately 2.5-fold. Using the MEG response as a surrogate for neuronal activity and predicting an fMRI response yields a 1.4-fold overprediction. This suggests that the nonlinearity that can be explained by transient onset activity cannot account for all of the nonlinearity in the fMRI response so there must be other hemodynamic nonlinearities or neuronal effects not accounted for in the MEG response.

## 4.2 Using nonlinearity to understand brain function

Utilizing an fMRI adaptation paradigm, we observed a release in adaptation in the orthogonal condition in visual areas V1, V2, V3, V3A, V4V, and MT+. We observed a release in adaptation for the opposite direction in only MT+. This is consistent with MT+ being direction-selective while visual areas V1, V2, V3, V3A, and V4V being orientation-selective. We also observed adaptation with presentation of the second stimulus suggesting that fMRI adaptation is affected by both neuronal and vascular components.

### 4.3 Future Experiments

Further studies employing both electrophysiological recordings and fMRI responses in identical paradigms will help elucidate the neuronal and vascular sources of the BOLD transient and adaptation signal. Since BOLD fMRI signal is a population response of underlying neurons, it makes most sense to record neuronal activity in cortical areas of interest without regard to specific tuning properties of the cell. That is, to obtain neuronal activity that is most representative of a cortical area, it is best to first place the electrode in the cortical area of interest and advance and record from random cells. This way, a truer sampling of the neuronal population occurs and can be used to correlate with the fMRI signal. Of course, a bias of picking up signals from larger neurons still occurs, but neurons should not be pre-selected on the basis of its tuning properties. While the ideal experiment would be simultaneous recording of fMRI and electrophysiological signals within a single brain, this is technically difficult to do and only one group has been able to achieve this (Logothetis et al. 2001). However, even cross-species comparison with human fMRI and non-human primate electrophysiological data using the identical paradigm would yield insights into the relative contributions of the neuronal and hemodynamic input into the fMRI signal.

## References

**Albrecht DG, Farrar SB, and Hamilton DB**. Spatial contrast adaptation characteristics of neurones recorded in the cat's visual cortex. *J Physiol (Lond)* 347: 713-739, 1984.

**Albright TD**. Direction and orientation selectivity of neurons in visual area MT of the macaque. *J Neurophysiol* 52: 1106-1130., 1984.

**Aron A, Fisher H, Mashek DJ, Strong G, Li H, and Brown LL**. Reward, motivation, and emotion systems associated with early-stage intense romantic love. *J Neurophysiol* 94: 327-337, 2005.

**Bandettini PA, Jesmanowicz A, Wong EC, and Hyde JS**. Processing strategies for time-course data sets in functional MRI of the human brain. *Magn Reson Med* 30: 161-173, 1993.

**Bandettini PA, Wong EC, Hinks RS, Tikofsky RS, and Hyde JS**. Time course EPI of human brain function during task activation. *Magn Reson Med* 25: 390-397, 1992.

**Belliveau JW, Kennedy DN, Jr., McKinstry RC, Buchbinder BR, Weisskoff RM, Cohen MS, Vevea JM, Brady TJ, and Rosen BR**. Functional mapping of the human visual cortex by magnetic resonance imaging. *Science* 254: 716-719, 1991.

**Birn RM and Bandettini PA**. The effect of stimulus duty cycle and "off" duration on BOLD response linearity. *Neuroimage* 27: 70-82, 2005.

**Birn RM, Saad ZS, and Bandettini PA**. Spatial heterogeneity of the nonlinear dynamics in the FMRI BOLD response. *Neuroimage* 14: 817-826, 2001.

**Bonds AB**. Temporal dynamics of contrast gain in single cells of the cat striate cortex. *Vis Neurosci* 6: 239-255, 1991.

**Boynton GM, Demb JB, Glover GH, and Heeger DJ**. Neuronal basis of contrast discrimination. *Vision Res* 39: 257-269, 1999.

**Boynton GM, Engel SA, Glover GH, and Heeger DJ**. Linear systems analysis of functional magnetic resonance imaging in human V1. *J Neurosci* 16: 4207-4221, 1996.

**Boynton GM and Finney EM**. Orientation-specific adaptation in human visual cortex. *J Neurosci* 23: 8781-8787, 2003.

**Brainard DH**. The Psychophysics Toolbox. *Spat Vis* 10: 433-436, 1997.

**Buckner RL**. Event-related fMRI and the hemodynamic response. *Hum Brain Mapp* 6: 373-377, 1998.

**Buracas GT and Boynton GM**. Efficient design of event-related fMRI experiments using M-sequences. *Neuroimage* 16: 801-813, 2002.

**Buracas GT, Fine I, and Boynton GM**. The relationship between task performance and functional magnetic resonance imaging response. *J Neurosci* 25: 3023-3031, 2005.

**Cannestra AF, Pouratian N, Shomer MH, and Toga AW**. Refractory periods observed by intrinsic signal and fluorescent dye imaging. *J Neurophysiol* 80: 1522-1532, 1998.

**Cohen MS**. Parametric analysis of fMRI data using linear systems methods. *Neuroimage* 6: 93-103, 1997.

**Cox RW**. AFNI: software for analysis and visualization of functional magnetic resonance neuroimages. *Comput Biomed Res* 29: 162-173, 1996.

**Dale AM and Buckner RL**. Selective averaging of rapidly presented individual trials using fMRI. *Human Brain Mapping* 5: 329-340, 1997.

**Doughty MJ**. Consideration of three types of spontaneous eyeblink activity in normal humans: during reading and video display terminal use, in primary gaze, and while in conversation. *Optom Vis Sci* 78: 712-725, 2001.

**Engel SA**. Adaptation of oriented and unoriented color-selective neurons in human visual areas. *Neuron* 45: 613-623, 2005.

**Engel SA and Furmanski CS**. Selective adaptation to color contrast in human primary visual cortex. *J Neurosci* 21: 3949-3954, 2001.

**Engel SA, Rumelhart DE, Wandell BA, Lee AT, Glover GH, Chichilnisky EJ, and Shadlen MN**. fMRI of human visual cortex. *Nature* 369: 525, 1994.

**Fang F, Murray SO, Kersten D, and He S**. Orientation-tuned FMRI adaptation in human visual cortex. *J Neurophysiol* 94: 4188-4195, 2005.

**Fawcett IP, Barnes GR, Hillebrand A, and Singh KD**. The temporal frequency tuning of human visual cortex investigated using synthetic aperture magnetometry. *Neuroimage* 21: 1542-1553, 2004.

**Fox MD, Snyder AZ, Barch DM, Gusnard DA, and Raichle ME**. Transient BOLD responses at block transitions. *Neuroimage* 28: 956-966, 2005a.

**Fox MD, Snyder AZ, McAvoy MP, Barch DM, and Raichle ME**. The BOLD onset transient: identification of novel functional differences in schizophrenia. *Neuroimage* 25: 771-782, 2005b.

**Friston KJ**. Bayesian estimation of dynamical systems: an application to fMRI. *Neuroimage* 16: 513-530, 2002.

**Friston KJ**. Imaging neuroscience: principles or maps? *Proc Natl Acad Sci U S A* 95: 796-802, 1998.

**Friston KJ, Frith CD, Liddle PF, and Frackowiak RS**. Comparing functional (PET) images: the assessment of significant change. *J Cereb Blood Flow Metab* 11: 690-699, 1991.

**Friston KJ and Henson RN**. Commentary on: Divide and conquer; a defence of functional localisers. *Neuroimage* 30: 1097-1099, 2006.

**Friston KJ, Mechelli A, Turner R, and Price CJ**. Nonlinear responses in fMRI: the Balloon model, Volterra kernels, and other hemodynamics. *Neuroimage* 12: 466-477, 2000.

**Friston KJ, Rotshtein P, Geng JJ, Sterzer P, and Henson RN**. A critique of functional localisers. *Neuroimage* 30: 1077-1087, 2006.

**Gandhi SP, Heeger DJ, and Boynton GM**. Spatial attention affects brain activity in human primary visual cortex. *Proc Natl Acad Sci U S A* 96: 3314-3319, 1999.

**Geisler WS and Albrecht DG**. Visual cortex neurons in monkeys and cats: detection, discrimination, and identification. *Vis Neurosci* 14: 897-919, 1997.

**Glover GH**. Deconvolution of impulse response in event-related BOLD fMRI. *Neuroimage* 9: 416-429, 1999.

**Goebel R, Esposito F, and Formisano E**. Analysis of functional image analysis contest (FIAC) data with brainvoyager QX: From single-subject to cortically aligned group general linear model analysis and self-organizing group independent component analysis. *Hum Brain Mapp* 27: 392-401, 2006.

**Goodyear BG, Zhu H, Brown RA, and Mitchell JR**. Removal of phase artifacts from fMRI data using a Stockwell transform filter improves brain activity detection. *Magn Reson Med* 51: 16-21, 2004.

**Grill-Spector K, Kushnir T, Edelman S, Avidan G, Itzchak Y, and Malach R**. Differential processing of objects under various viewing conditions in the human lateral occipital complex. *Neuron* 24: 187-203, 1999.

**Grill-Spector K and Malach R**. fMR-adaptation: a tool for studying the functional properties of human cortical neurons. *Acta Psychol (Amst)* 107: 293-321, 2001.

**Heeger DJ, Huk AC, Geisler WS, and Albrecht DG**. Spikes versus BOLD: what does neuroimaging tell us about neuronal activity? *Nat Neurosci* 3: 631-633., 2000.

**Heeger DJ and Ress D**. What does fMRI tell us about neuronal activity? *Nat Rev Neurosci* 3: 142-151, 2002.

**Hubel DH and Wiesel TN**. Receptve field, binocular interactions and functional architecture in the cat's visual cortex. *J Physiol (Lond)* 160: 106–154, 1962.

**Huettel SA and McCarthy G**. Evidence for a refractory period in the hemodynamic response to visual stimuli as measured by MRI. *Neuroimage* 11: 547-553., 2000.

**Huettel SA and McCarthy G**. Regional differences in the refractory period of the hemodynamic response: an event-related fMRI study. *Neuroimage* 14: 967-976, 2001.

**Huettel SA, Obembe OO, Song AW, and Woldorff MG**. The BOLD fMRI refractory effect is specific to stimulus attributes: evidence from a visual motion paradigm. *Neuroimage* 23: 402-408, 2004.

**Huk AC, Ress D, and Heeger DJ**. Neuronal basis of the motion aftereffect reconsidered. *Neuron* 32: 161-172, 2001.

**Illes J, Kirschen MP, and Gabrieli JD**. From neuroimaging to neuroethics. *Nat Neurosci* 6: 205, 2003.

**Inan S, Mitchell T, Song A, Bizzell J, and Belger A**. Hemodynamic correlates of stimulus repetition in the visual and auditory cortices: an fMRI study. *Neuroimage* 21: 886-893, 2004.

**Kohn A and Movshon JA**. Adaptation changes the direction tuning of macaque MT neurons. *Nat Neurosci* 7: 764-772, 2004.

**Kohn A and Movshon JA**. Neuronal adaptation to visual motion in area MT of the macaque. *Neuron* 39: 681-691, 2003.

**Kourtzi Z and Huberle E**. Spatiotemporal characteristics of form analysis in the human visual cortex revealed by rapid event-related fMRI adaptation. *Neuroimage* 28: 440-452, 2005.

**Kourtzi Z and Kanwisher N**. Representation of perceived object shape by the human lateral occipital complex. *Science* 293: 1506-1509, 2001.

**Kourtzi Z, Tolias AS, Altmann CF, Augath M, and Logothetis NK**. Integration of local features into global shapes: monkey and human FMRI studies. *Neuron* 37: 333-346, 2003.

**Krekelberg B, Boynton GM, and van Wezel RJ**. Adaptation: from single cells to BOLD signals. *Trends Neurosci* 29: 250-256, 2006a.

**Krekelberg B, van Wezel RJ, and Albright TD**. Adaptation in macaque MT reduces perceived speed and improves speed discrimination. *J Neurophysiol* 95: 255-270, 2006b.

**Krekelberg B, Vatakis A, and Kourtzi Z**. Implied motion from form in the human visual cortex. *J Neurophysiol* 94: 4373-4386, 2005.

**Kwong KK, Belliveau JW, Chesler DA, Goldberg IE, Weisskoff RM, Poncelet BP, Kennedy DN, Hoppel BE, Cohen MS, Turner R, and et al.** Dynamic magnetic resonance imaging of human brain activity during primary sensory stimulation. *Proc Natl Acad Sci U S A* 89: 5675-5679, 1992.

**Larsson J, Landy MS, and Heeger DJ**. Orientation-selective adaptation to first- and second-order patterns in human visual cortex. *J Neurophysiol* 95: 862-881, 2006.

**Lin FH, Witzel T, Hamalainen MS, Dale AM, Belliveau JW, and Stufflebeam SM**. Spectral spatiotemporal imaging of cortical oscillations and interactions in the human brain. *Neuroimage* 23: 582-595, 2004.

**Logothetis NK, Pauls J, Augath M, Trinath T, and Oeltermann A**. Neurophysiological investigation of the basis of the fMRI signal. *Nature* 412: 150-157., 2001.

**Maddess T, McCourt ME, Blakeslee B, and Cunningham RB**. Factors governing the adaptation of cells in area-17 of the cat visual cortex. *Biol Cybern* 59: 229-236, 1988.

**Mathiesen C, Caesar K, Akgoren N, and Lauritzen M**. Modification of activity-dependent increases of cerebral blood flow by excitatory synaptic activity and spikes in rat cerebellar cortex. *J Physiol* 512 ( Pt 2): 555-566, 1998.

**Mechelli A, Price CJ, and Friston KJ**. Nonlinear coupling between evoked rCBF and BOLD signals: a simulation study of hemodynamic responses. *Neuroimage* 14: 862-872, 2001.

**Miller KL, Luh WM, Liu TT, Martinez A, Obata T, Wong EC, Frank LR, and Buxton RB**. Nonlinear temporal dynamics of the cerebral blood flow response. *Hum Brain Mapp* 13: 1-12., 2001.

**Movshon JA and Lennie P**. Pattern-selective adaptation in visual cortical neurones. *Nature* 278: 850-852, 1979.

**Muller JR, Metha AB, Krauskopf J, and Lennie P**. Information conveyed by onset transients in responses of striate cortical neurons. *J Neurosci* 21: 6978-6990, 2001.

**Muller JR, Metha AB, Krauskopf J, and Lennie P**. Rapid adaptation in visual cortex to the structure of images. *Science* 285: 1405-1408, 1999.

**Murray SO, Olman CA, and Kersten D**. Spatially specific FMRI repetition effects in human visual cortex. *J Neurophysiol* 95: 2439-2445, 2006.

**Murray SO and Wojciulik E**. Attention increases neural selectivity in the human lateral occipital complex. *Nat Neurosci* 7: 70-74, 2004.

**Obata T, Liu TT, Miller KL, Luh WM, Wong EC, Frank LR, and Buxton RB**. Discrepancies between BOLD and flow dynamics in primary and supplementary motor areas: application of the balloon model to the interpretation of BOLD transients. *Neuroimage* 21: 144-153, 2004.

**Ogawa S, Tank DW, Menon R, Ellermann JM, Kim SG, Merkle H, and Ugurbil K**. Intrinsic signal changes accompanying sensory stimulation: functional brain mapping with magnetic resonance imaging. *Proc Natl Acad Sci U S A* 89: 5951-5955, 1992.

**Ohzawa I, Sclar G, and Freeman RD**. Contrast gain control in the cat's visual system. *J Neurophysiol* 54: 651-667, 1985.

**Pelli DG**. The VideoToolbox software for visual psychophysics: transforming numbers into movies. *Spat Vis* 10: 437-442, 1997.

**Penny W and Friston K**. Mixtures of general linear models for functional neuroimaging. *IEEE Trans Med Imaging* 22: 504-514, 2003.

**Petersen SE, Baker JF, and Allman JM**. Direction-specific adaptation in area MT of the owl monkey. *Brain Res* 346: 146-150, 1985.

**Pfeuffer J, McCullough JC, Van de Moortele PF, Ugurbil K, and Hu X**. Spatial dependence of the nonlinear BOLD response at short stimulus duration. *Neuroimage* 18: 990-1000, 2003.

**Rao SM, Binder JR, Bandettini PA, Hammeke TA, Yetkin FZ, Jesmanowicz A, Lisk LM, Morris GL, Mueller WM, Estkowski LD, and et al.** Functional magnetic resonance imaging of complex human movements. *Neurology* 43: 2311-2318, 1993.

**Rees G, Friston K, and Koch C**. A direct quantitative relationship between the functional properties of human and macaque V5. *Nat Neurosci* 3: 716-723., 2000.

**Robson MD, Dorosz JL, and Gore JC**. Measurements of the temporal fMRI response of the human auditory cortex to trains of tones. *Neuroimage* 7: 185-198, 1998.

**Saxe R, Brett M, and Kanwisher N**. Divide and conquer: A defense of functional localizers. *Neuroimage* 30: 1088-1096, 2006.

**Sereno MI, Dale AM, Reppas JB, Kwong KK, Belliveau JW, Brady TJ, Rosen BR, and Tootell RB**. Borders of multiple visual areas in humans revealed by functional magnetic resonance imaging. *Science* 268: 889-893, 1995.

**Sereno MI, McDonald CT, and Allman JM**. Analysis of retinotopic maps in extrastriate cortex. *Cereb Cortex* 4: 601-620, 1994.

**Tolias AS, Keliris GA, Smirnakis SM, and Logothetis NK**. Neurons in macaque area V4 acquire directional tuning after adaptation to motion stimuli. *Nat Neurosci* 8: 591-593, 2005.

**Tootell RB, Hadjikhani NK, Vanduffel W, Liu AK, Mendola JD, Sereno MI, and Dale AM**. Functional analysis of primary visual cortex (V1) in humans. *Proc Natl Acad Sci U S A* 95: 811-817, 1998.

**Van Wezel RJ and Britten KH**. Motion adaptation in area MT. *J Neurophysiol* 88: 3469-3476, 2002.

**Vazquez AL and Noll DC**. Nonlinear aspects of the BOLD response in functional MRI. *Neuroimage* 7: 108-118, 1998.